

AEDC-TR-71-254

9.2

JAN 3 1972

MAY 12 1972

SEP 20 1978

FEB 16 1983

SEP 13 1984



SIMULATION OF THE IONOSPHERE UTILIZING MICROWAVE ION GENERATION TECHNIQUES

M. R. Busby and B. W. Gilley

ARO, Inc.

December 1971

**TECHNICAL REPORTS
FILE COPY**

Approved for public release; distribution unlimited.

**VON KÁRMÁN GAS DYNAMICS FACILITY
ARNOLD ENGINEERING DEVELOPMENT CENTER
AIR FORCE SYSTEMS COMMAND
ARNOLD AIR FORCE STATION, TENNESSEE**

PROPERTY OF U S AIR FORCE
AEDC LIBRARY
F40600-72-C-0003

NOTICES

When U. S. Government drawings specifications, or other data are used for any purpose other than a definitely related Government procurement operation, the Government thereby incurs no responsibility nor any obligation whatsoever, and the fact that the Government may have formulated, furnished, or in any way supplied the said drawings, specifications, or other data, is not to be regarded by implication or otherwise, or in any manner licensing the holder or any other person or corporation, or conveying any rights or permission to manufacture, use, or sell any patented invention that may in any way be related thereto.

Qualified users may obtain copies of this report from the Defense Documentation Center.

References to named commercial products in this report are not to be considered in any sense as an endorsement of the product by the United States Air Force or the Government.

SIMULATION OF THE IONOSPHERE UTILIZING
MICROWAVE ION GENERATION TECHNIQUES

M. R. Busby and B. W. Gilley
ARO, Inc.

Approved for public release; distribution unlimited.

FOREWORD

The research reported herein was sponsored by the Arnold Engineering Development Center (AEDC), Air Force Systems Command (AFSC), Arnold Air Force Station, Tennessee, in support of Program Element 64719F.

The results of the research were obtained by ARO, Inc. (a subsidiary of Sverdrup & Parcel and Associates, Inc.), contract operator of the AEDC, AFSC, under Contract F40600-72-C-0003. The research was conducted from March to June 1971, under ARO Project No. VW3126. The manuscript was submitted for publication on September 29, 1971.

This technical report has been reviewed and is approved.

Michael G. Buja
Captain, USAF
Research and Development
Division
Directorate of Technology

Robert O. Dietz
Acting Director
Directorate of
Technology

ABSTRACT

An experimental investigation of the simulation of the environment encountered in the lower regions of the ionosphere (50 to 500 km) has been conducted at AEDC. Microwave cavities were utilized in conjunction with a converging-diverging nozzle and a cryogenically pumped vacuum chamber to produce supersonic flow fields with small ion number densities. A platinum, cylindrical, electrostatic probe was used to measure the voltage-current characteristics of the low density plasma in the nozzle exit plane. For exit plane Mach numbers of 2.86 to 3.17, ion densities of $5.75 \times 10^5 \text{ cm}^{-3}$ to $1.69 \times 10^6 \text{ cm}^{-3}$ and electron temperatures of $3000^\circ\text{K} \pm 900^\circ\text{K}$ were calculated using the electrostatic probe characteristics.

CONTENTS

	<u>Page</u>
ABSTRACT	iii
I. INTRODUCTION	1
II. EXPERIMENTAL APPARATUS	
2.1 Research Vacuum Chamber and Conical Nozzle	1
2.2 Ion Generation.	2
2.3 Electrostatic Probe	2
III. ELECTROSTATIC PROBE THEORY	3
IV. EXPERIMENTAL PROCEDURE	
4.1 Calibration of the Supersonic Nozzle	8
4.2 Operational Procedure for Ion Density Measure- ment	9
V. EXPERIMENTAL RESULTS	
5.1 Ion Density Profiles	9
5.2 Estimation of the Electron Temperature	10
5.3 Conclusions	10
REFERENCES	11

APPENDIXES

I. ILLUSTRATIONS

Figure

1. Typical Electron Distributions in the Ionosphere	15
2. Research Vacuum Chamber	16
3. Mach Number 3 Conical Nozzle	17
4. Gas Addition System and Microwave Generators.	18
5. Schematic of the Electrostatic Probe Instrumentation	19
6. Electrostatic Probe Instrumentation and Vacuum Cell	20
7. Path of a Charged Particle Passing through a Sheath Surrounding a Cylinder	21
8. Total Mass Flow as a Function of Plenum Pressure for the Mach Number 3 Conical Nozzle	22
9. Pitot Tube Viscous Effect.	23

<u>Figure</u>	<u>Page</u>
10. Mach Number 3 Nozzle Calibration	24
11. Pitot Pressure Profiles in Nozzle Exit Plane.	25
12. Nozzle Exit Plane Core Diameter for Various Plenum Pressures	26
13. Voltage-Current Characteristics for Various Probe Positions in Nozzle Exit Plane	27
14. I^2 -V Curves for Mach Number 3.17 and 100-percent Microwave Power	28
15. I^2 -V Curves for Mach Number 3.17 and 75-percent Microwave Power	29
16. I^2 -V Curves for Mach Number 3.17 and 50-percent Microwave Power	30
17. I^2 -V Curves for Mach Number 3.06 and 100-percent Microwave Power	31
18. I^2 -V Curves for Mach Number 3.06 and 50-percent Microwave Power	32
19. I^2 -V Curves for Mach Number 2.91 and 100-percent Microwave Power	33
20. I^2 -V Curves for Mach Number 2.91 and 50-percent Microwave Power	34
21. I^2 -V Curves for Mach Number 2.86 and 100-percent Microwave Power	35
22. I^2 -V Curves for Mach Number 2.86 and 50-percent Microwave Power	36
23. Normalized Exit Plane Ion Density Profiles for Mach Number 3.17	37
24. Normalized Exit Plane Ion Density Profiles for Mach Number 3.06	38
25. Normalized Exit Plane Ion Density Profiles for Mach Number 2.91	39
26. Normalized Exit Plane Ion Density Profiles for Mach Number 2.86	40
27. Nozzle Exit Plane I-V Curves for Various Probe Positions	41

<u>Figure</u>		<u>Page</u>
28.	Nozzle Exit Plane I-V Curves for Various Mach Numbers	42
29.	Nozzle Exit Plane I-V Curves for Various Microwave Powers	43

II. TABLES

I.	Characteristics of the Ionosphere	44
II.	Centerline Ion Densities in the Nozzle Exit Plane for Various Microwave Powers	44
III.	Estimated Electron Temperatures in the Nozzle Exit Plane for Mach Number ≈ 3.17	45
IV.	Estimated Centerline Electron Temperatures for Various Mach Numbers in the Nozzle Exit Plane	45
V.	Estimated Centerline Electron Temperatures for Various Values of Microwave Power in the Nozzle Exit Plane	46
IV.	Comparison of Experimental Results with Desired Ionosphere Conditions	46

SECTION I INTRODUCTION

In recent years there has been considerable interest (for example, from the Air Force Cambridge Research Laboratory) in a ground-based facility capable of generating conditions corresponding to those in the ionosphere. Such a facility could be conveniently utilized in the calibration of atmospheric electrostatic sampling probes which attempt to determine ion concentrations and electron temperatures in the upper atmosphere. The conditions for which simulation is desired are (1) altitudes from 50 to 500 km, (2) Mach numbers from 2 to 5, and (3) ion densities from 10^3 to 10^6 per cc. The attempt to attain these conditions simultaneously in a ground test facility is the subject of this report.

The upper atmosphere is an extremely rarefied, partially ionized gas. The concentration of neutral particles, molecules, and atoms decreases sharply with increasing altitude (Ref. 1). For example, at 100 km there are approximately 10^{13} particles/cm³, whereas at an altitude of 1000 km there are approximately 10^5 particles/cm³ (Table I, Appendix II). In the lower regions of the ionosphere, the concentrations of ions and electrons vary strongly, not only with altitude (Fig. 1, Appendix I) but also with the time of year and during a 24-hr period (Ref. 2). With increasing height, the concentrations of ions and electrons decrease considerably slower than the molecular concentration. Accordingly, the degree of ionization of the ionosphere increases with increasing height. For example, at an altitude of 100 km, the plasma is very weakly ionized; the ratio of ions to neutrals (N_o/n_o) amounts to only 10^{-8} to 10^{-10} . At an altitude of 300 km the ratio $N_o/n_o \approx 10$, and at 3000 km the ratio N_o/n_o is approximately 10^4 . In this report the simulation of the lower ionosphere (50 to 500 km), corresponding to conditions which would be encountered by gages, electrostatic probes, and other devices mounted in sounding rockets, is discussed.

SECTION II EXPERIMENTAL APPARATUS

2.1 RESEARCH VACUUM CHAMBER AND CONICAL NOZZLE

The vacuum chamber used in these experiments is a stainless steel cylinder 4 ft in diameter and 10 ft long (Fig. 2). The chamber is equipped with a 300-cfm Stokes mechanical pump which is used to rough the cell down to a pressure of approximately 20 μ Hg. Chamber pressures in the

10^{-6} torr range are achieved by a 6-in. oil diffusion pump backed by a 13-cfm Welch mechanical pump. The chamber is also equipped with a liquid-nitrogen-cooled cryoliner (77°K) and a finned aluminum gaseous-helium-cooled cryopump (20°K). When cryogenic cooling is used, a base pressure of 5×10^{-9} torr is achieved in the chamber. A miniature GE ionization gage is located in the aft portion of the chamber and is used to monitor the static pressure in this region (Fig. 2). An Alphatron® gage is located in the plenum chamber and is used to record the stagnation pressure.

A stainless steel conical Mach 3 nozzle is located at the forward end of the chamber with an exit diameter of 20 in. and throat diameter of 7.1 in. The overall length of the nozzle is 37 in. (Fig. 3). The throat and divergent portion of the nozzle are cooled by a liquid-nitrogen jacket.

2.2 ION GENERATION

Three Raytheon PGM-10 microwave power generators featuring magnetron oscillators were used to ionize a portion of the gas flow into the plenum chamber. Nitrogen gas from a high-pressure bottle was admitted to the plenum chamber through a manifold of three 0.5-in.-diam quartz tubes (Fig. 4). Each tube passed through a tunable microwave cavity where energy from the generators was applied to the gas. Each generator is capable of supplying power output in excess of 85 watts at a frequency of 2450 mHz. Power output is continuously adjustable by means of a variable auto-transformer which controls the voltage applied to the magnetron.

2.3 ELECTROSTATIC PROBE

The electrostatic probe used to determine ion densities was a 0.508-cm-diam platinum rod which was inserted in a glass tube, leaving approximately 7 cm of its length exposed. The glass tube probe support was attached to the side of the pitot probe traversing mechanism within the research vacuum chamber. Teflon® insulated wire was used to connect the probe to instrumentation outside the chamber.

A block diagram of the electrostatic probe instrumentation is shown as Fig. 5, and a photograph of the vacuum chamber and instrumentation is presented in Fig. 6. Sweep voltage, furnished by a Wavetec® function generator, was a triangular wave of approximately ± 15 volts. A Boonton Model 95A sensitive d-c meter was used to measure and amplify the

small probe currents. The meter output, a voltage proportional to input current, was applied to the Y-axis of a Moseley X-Y plotter. Sweep voltage from the function generator was applied to the X-axis, producing current versus voltage graphs of the probe characteristic on the plotter. Isolation plugs were used with all instruments so that the only ground connection was to the test chamber.

SECTION III ELECTROSTATIC PROBE THEORY

A great deal of information regarding the nature of a plasma flow field can be obtained from the voltage-current characteristics of an electrostatic probe immersed in the charged region. The following discussion is a summary of the probe theory presented by Langmuir and Mott-Smith (Ref. 3). When a collector is negatively charged, it repels electrons from its neighborhood but gathers positive ions. It thus becomes surrounded by a positive ion sheath which contains a positive ion space charge but no free electrons. The whole drop in potential between the ionized gas and the collector becomes concentrated within this sheath, the positive space charge on the ions in the sheath being able to neutralize the effect of the negative charge on the electrode so that the field of the collector does not extend beyond the outer edge of the sheath. The number of ions taken up by the collector is thus limited by the number that reaches the outer edge of the sheath as a result of their proper motions. The current density over the area of the outside of the sheath measures the positive ion current density in the ionized gas.

In a similar manner, a positively charged probe becomes surrounded by an electron sheath, and the current is limited by the rate at which the electrons reach the edge of the sheath; and in this manner, the electron current density in the ionized gas may be measured. Because of the small mass and high mobility of electrons, the electron current densities in uniformly ionized plasmas are hundreds of times greater than the positive ion current densities. In measuring electron current densities there is a limit to the positive voltage that may be used on the collector, since ionization by collision becomes significant at a certain voltage. Too, the positive ions produced within the sheath neutralize the electron space charge and allow the current to increase indefinitely without further increase in voltage.

If the collector is at a potential slightly negative with respect to the space, electrons may still reach the probe if they have sufficient

velocities to carry them against the retarding field which they encounter within the positive ion sheath. As the collector is made more negative, the lower speed electrons fail to reach the collector, while those with high speed may still reach it. The current-voltage characteristic of a probe thus gives indications as to the distribution of velocities among the electrons in the ionized gas.

When the electron velocities have a Maxwellian distribution, the electron current, i , flowing to any collector at a potential V , which is negative with respect to the surrounding space, is given by the equation

$$i = IA \exp \{Ve/(kT)\} \quad (1)$$

where I is the electron current density in the ionized gas, A is the surface area of the probe, e is the charge on the electron, k is the Boltzmann constant (1.372×10^{-16} erg/°K), and T is the absolute temperature corresponding to the velocity distribution of the electrons. If V is expressed in volts, the value of e/k becomes 11,600°K/volt.

Equation (1) does not apply when the potential of the collector is such as to exert an attractive force on the particles being collected. For an accelerating field, the apparent increase in current density near the probe (in the sheath region) as compared with that farther from it, is attributed to the large number of low-velocity electrons, resulting from collisions, which are trapped within the region around the collector by the accelerating field which prevents their escape. With low intensities of ionization, the diameter of the sheath may be many times greater than that of the collector. The initial velocities of the electrons or ions as they enter the sheath may thus cause them to form orbits which carry them out of the sheath again without colliding with the collector.

When the sheath radius is large compared to that of the collector, and especially when the initial velocities of the electrons or ions are high, the orbital motion of the particles must be considered. Let the small circle about F in Fig. 7 represent the cross section of a cylindrical probe charged, for example, negatively with respect to the surrounding space. The field produced by the probe extends only within a region of radius a , indicated in the illustration by the dotted circle. Consider an ion of mass m moving with a velocity v_0 along a path AB and let BC be the extension of the straight line AB . Then the angular momentum of the ion about F is equal to mv_0p_0 where p_0 is the perpendicular distance OF from the line AC to the axis or center of the probe.

The force exerted on the ion by the probe will cause the ion to move along some such path as $ABMDE$, the portions AB and DE being straight.

At some point M, the ion will be at a minimum distance p_m from the center of the probe, and at this point the velocity v_m of the ion is wholly tangential. Since the probe can exert only a central force on the ion, the angular momentum about F must remain constant throughout the path. Thus, one may place

$$mv_0 p_0 = mv_m p_m \quad (2)$$

It is convenient to express the velocities of ions in terms of the potential differences necessary to produce them. The work done on an ion in moving through a potential difference V is Ve , and this is equal to the gain in kinetic energy so that

$$1/2 mv^2 = Ve \quad (3)$$

Combining this with Eq. (2), one obtains

$$V_0 p_0^2 = V_m p_m^2 \quad (4)$$

where V_0 measures the initial kinetic energy of the ion in volts and V_m is the corresponding energy when at the minimum distance from F. As the potential is increased on the probe, the ion is deflected further so that p_m decreases.

When $p_m = r$, the radius of F, the ion makes a grazing collision with the surface of the probe. If V is the potential of the probe, then the energy of the ion at the moment of collision is measured by $V_0 + V$. Substituting this for V_m in Eq. 4 and placing $p_m = r$, one obtains

$$p_{0 \max} = r \sqrt{1 + V/V_0} \quad (5)$$

In order that any ion may reach the probe, the value of p_0 for its path must be less than the value of $p_{0 \max}$ given by Eq. 5. Thus, p is the radius of the "effective target" of the probe. Therefore, if I is the current density of the ions, the current, i , taken up by a probe of surface area A for a cylindrical collector is

$$i = AI \sqrt{1 + V/V_0} \quad (6)$$

The equations are equally applicable to the collection of electrons. The problem of calculating the current under practical conditions is more difficult since the ions do not all have the same initial velocity as was assumed in deriving Eq. (6), but rather have velocities distributed by Maxwell's law. The complete mathematical solution of this problem has been worked out for cylinders by Langmuir and Mott-Smith.

For accelerating fields, the solution for cylinders of surface area A is

$$i = AIf \quad (7)$$

the function f being given by

$$f = (a/r)P(\sqrt{\phi}) + e^{\eta} \{1 - P(\sqrt{\eta + \phi})\}$$

where

$$\begin{aligned} \eta &= Ve/(kT) \\ \phi &= \frac{r^2}{a^2 - r^2} \eta \\ \eta + \phi &= \frac{a^2}{a^2 - r^2} \eta \end{aligned}$$

Here P stands for the probability integral defined by

$$P(x) = \frac{2}{\sqrt{\pi}} \int_0^x e^{-y^2} dy$$

The symbols V , e , k , T , a , and r have the meanings already assigned.

With low current densities, probes of small radius, and high initial velocities of the ions, the sheath radius becomes large compared to that of the probe. For this case, one may obtain from Eq. (7) a more convenient equation by assuming a/r is large compared to unity and expanding the resulting equation as a reciprocal power series in a/r which gives

$$f = (2/\sqrt{\pi})\sqrt{\eta + 1} \quad (8)$$

Substituting this into Eq. (7) and squaring, one obtains

$$i^2 = \frac{4 A^2 I^2}{\pi} (Ve/(kT) + 1) \quad (9)$$

Therefore, if the square of the observed current, i , is plotted against the potential of the collector, a straight line should be obtained. If S is the slope of this line, one has

$$S = \frac{4 A^2 I^2 e}{\pi kT}$$

or

$$I/\sqrt{T} = \sqrt{\pi k/4e} \sqrt{S/A} = 0.00822 \sqrt{S/A} \text{ amp cm}^{-2} \text{ deg}^{-1/2} \quad (10)$$

The intercept of the straight line on the V-axis is obtained from Eq. (9) by placing $i = 0$ and corresponds to a value of V given by

$$V_{i=0} = -kT/e = -T/11,600 \text{ volts}$$

Thus, the straight line represented by Eq. (9) crosses the V-axis at a point $T/11,600$ volts negative with respect to the potential of the space around the probe.

From the slope S one may calculate directly the number of ions (or electrons) per unit volume. The average velocity v of the ions, given by the kinetic theory, is

$$v = \sqrt{\frac{8kT}{\pi m}}$$

and the number of ions, n , corresponding to a current density I, per second per unit area passing a plane is given by

$$n = \frac{4I}{ve}$$

Substituting, one obtains an expression for the number density,

$$n = \sqrt{\frac{2\pi m}{kT}} I/e = 4.03 \times 10^{13} (I/\sqrt{T}) \sqrt{m/m_e}$$

and combining with Eq. (10),

$$n = \frac{\pi}{\sqrt{2e/m}} \sqrt{S/A} e = 3.32 \times 10^{11} (\sqrt{S/A}) \sqrt{m/m_e} \quad (11)$$

if \sqrt{S} is expressed in amp volt^{-1/2}.

Near the space potential, the square of the current will no longer follow the straight line law since the function f is not accurately represented by Eq. (8) in this region.

In the following sections, these equations will be applied to the experimental data obtained with the small platinum probe in a low density nitrogen flow. Since the cylindrical probe used in these studies was aligned with its axis parallel to the flow, the effects of flow velocity can be ignored (Ref. 4).

If the electrons in the charged flow field have a Maxwellian distribution, the electron temperature may be determined from Eq. (1) with the electrostatic probe being operated in the retarding potential region, that is, where the current-voltage characteristic gives an indication of the distribution of electron velocities. Taking the natural logarithm of both members of Eq. (1), one obtains

$$\ln i = \text{const} + V_e/(k T) \quad (12)$$

Thus, if the logarithm of the electron current i is plotted as a function of the probe potential V , a straight line of slope $e/(k T)$ should be obtained. Thus, the electron temperature in degrees Kelvin may be determined from

$$T = 5040/s \text{ } ^\circ\text{K} \quad (13)$$

where s is the slope on semilog base 10 paper.

SECTION IV EXPERIMENTAL PROCEDURE

4.1 CALIBRATION OF THE SUPERSONIC NOZZLE

The calibration of the nozzle exit flow was made with a 2.5-cm-diam pitot tube in the conventional manner. For various plenum pressures, P_0 , and stagnation temperatures, T_0 , the total mass flow (Fig. 8) and pitot pressures were recorded. The inviscid stagnation pressure, P'_0 , was determined by iterating with the pitot viscous effect function (Fig. 9) from Ref. 5. The ratio P'_0/P_0 which is a unique function of the Mach number was then determined and the free-stream Mach number obtained. Using the Mach number, plenum pressure, and stagnation temperature the free-stream properties may be calculated. Figure 10 presents the corrected values of Mach number for various values of plenum pressure for a stagnation temperature of 290°K and a nozzle wall temperature of 77°K.

To determine the variation of stream uniformity, the pitot tube was traversed across the flow field. Figure 11 presents the pitot pressure at various positions across the stream in the nozzle exit plane for various stagnation pressures. The variation of core diameter with stagnation pressure is presented in Fig. 12.

4.2 OPERATIONAL PROCEDURE FOR ION DENSITY MEASUREMENT

Ionized gas flow was generated at various levels of plenum pressure and microwave power. Values for relative microwave power were taken from the percent-of-power meters on each generator. The generators were individually set for the same percent-of-power output. A Tesla coil was used to initiate ionization in each cavity, and once initiated it was easily maintained over a wide range of power. Tuning of the microwave cavities was accomplished with the aid of a reflected power meter. Each cavity was adjusted for minimum standing wave ratio.

In addition to ions, the microwave cavities also produce not only other excited species but also dissociation in the test gas. The effects of these products in terms of ionospheric simulation have not been considered in this report.

The platinum, cylindrical probe previously described was used to obtain the voltage-current characteristic of the ionized gas in the nozzle exit plane. The axis of the probe was parallel to the nozzle axial centerline and the probe was traversed across the stream while data were taken at various stations.

Voltage applied to the probe was swept slowly (0.01 Hz) to avoid problems with the d-c meter used to read current. Frequency response of the meter amplifier is 3 db down at 1 Hz. There was a noticeable lag in meter output if sweep rates greater than 0.1 Hz were attempted.

SECTION V EXPERIMENTAL RESULTS

5.1 ION DENSITY PROFILES

The ion density was determined from Eq. (11) since the current-voltage characteristic was described by Eq. (9). Thus, the flow conditions were such that orbital motions of the electrons and ions were significant. A typical example of the current-voltage characteristics at various exit plane locations for a plenum pressure of 120 μ Hg is shown in Fig. 13. Negative values of length are the distances measured left of the nozzle centerline, whereas positive values are measured to the right of centerline. From these curves, graphs of the square of the ion current versus probe voltage were constructed. A complete set of these plots for the various flow conditions is presented in Figs. 14 through 22.

Since the current is determined by orbital motion, the square of the current when plotted versus the probe voltage gives a line nearly straight. The deviation of the points from a straight line is caused by the arrival of electrons. The slopes of these lines were determined and the ion number density calculated. Normalized ion density profiles for various flow conditions and microwave cavity power are presented in Figs. 23 through 26. Centerline ion densities ranged from 5.75×10^5 to 1.69×10^6 ion/cm³ for Mach numbers of 2.86 to 3.17, respectively. In all cases, the ion profiles were narrower than the corresponding pitot pressure profiles. Also, the centerline ion densities increased as the microwave power decreased, as shown in Table II. One possible explanation for this increase is that as the microwave power increases, the efficiency of ion generation may decrease because of a change in the properties of the plasma, for example, the plasma impedance. This decrease in ion generation rate would result in smaller exit plane ion densities, thus giving the observed results.

5.2 ESTIMATION OF THE ELECTRON TEMPERATURE

The electron temperatures were estimated using Eq. (13) after determining the values of the slope, s , from a semilogarithmic plot of the current-voltage characteristics. Figures 27 through 29 present these graphs for various flow conditions. Table III presents the estimated values of the electron temperature at various probe positions, Table IV gives T for various Mach numbers, and Table V presents T for several values of microwave power. An examination of these tables reveals a great deal of scatter in the estimation of the electron temperature. For the test conditions used in this investigation, the value of T should be essentially constant. The scatter is attributed primarily to the difficulty in replotting the data from the current-voltage characteristic onto the semilogarithmic graph. An average of the estimated values of the electron temperatures gives 3000°K for T . The smallest calculated value of T was 2180°K (Table V), whereas the largest value was 3980°K (Table III). Thus, the value of electron temperature in this report is taken to be 3000°K \pm 900°K.

5.3 CONCLUSIONS

The feasibility of the use of microwave cavities for the production of low density ionized flows has been demonstrated. Measurements of the characteristics of the neutral flow were carried out using a pitot probe, and having applied the appropriate viscous corrections, the neutral flow Mach number and density were determined. A cylindrical, platinum

electrostatic probe with its axis aligned parallel to the nozzle axial centerline was used to record the current-voltage characteristics of the partially ionized gas. The flow conditions were such that the orbital motions of the ions and electrons were significant, and the appropriate equations were derived and used to reduce the experimental data. Centerline exit plane ion densities of 5.75×10^5 ions/cm³ to 1.69×10^6 ions/cm³ for Mach numbers of 2.86 to 3.17, respectively, were measured with estimated electron temperatures of $3000^\circ\text{K} \pm 900^\circ\text{K}$. In all cases investigated, the ion density profiles were narrower than the corresponding pitot pressure profiles. Table VI presents a comparison of the desired ionosphere flow characteristics and those actually measured in the experiment. The simulation of the ionosphere flow properties is good, as shown in Table VI, although the experimental value of the neutral density and electron temperature is somewhat higher than those desired. This experimental study has only been preliminary, and further work is required (for example, calibration using other electrostatic probes and sophistication and improvement of the data acquisition techniques) in order to provide an ionospheric simulation facility for the ground testing of rocket-borne atmospheric probes, gages, and other devices.

REFERENCES

1. Al'pert, Y. L., Gurevich, A. V., and Pitaevskii, L. P. Space Physics with Artificial Satellites. Consultants Bureau, New York, Vol. 2, 1965.
2. de Leeuw, J. H. "A Brief Introduction to Ionospheric Aerodynamics." Rarefied Gas Dynamics, Fifth Symposium, Academic Press, Inc., New York, Vol. 2, 1967, pp. 1561-1586.
3. Langmuir, I. and Mott-Smith, H. "Studies of Electric Discharges in Gases at Low Pressures." The Collected Works of Irving Langmuir, Pergamon Press, New York, Vol. 4, 1961, pp. 23-98.
4. Clayden, W. A. "Review of Electrostatic Probes." R. A. R. D. E. Memorandum 32/68, 1968, p. 12.
5. Whitfield, D. L. and Stephenson, W. B. "Sphere Drag in the Free-Molecular and Transition Flow Regimes." AEDC-TR-70-32 (AD704122), April 1970.

APPENDIXES
I. ILLUSTRATIONS
II. TABLES

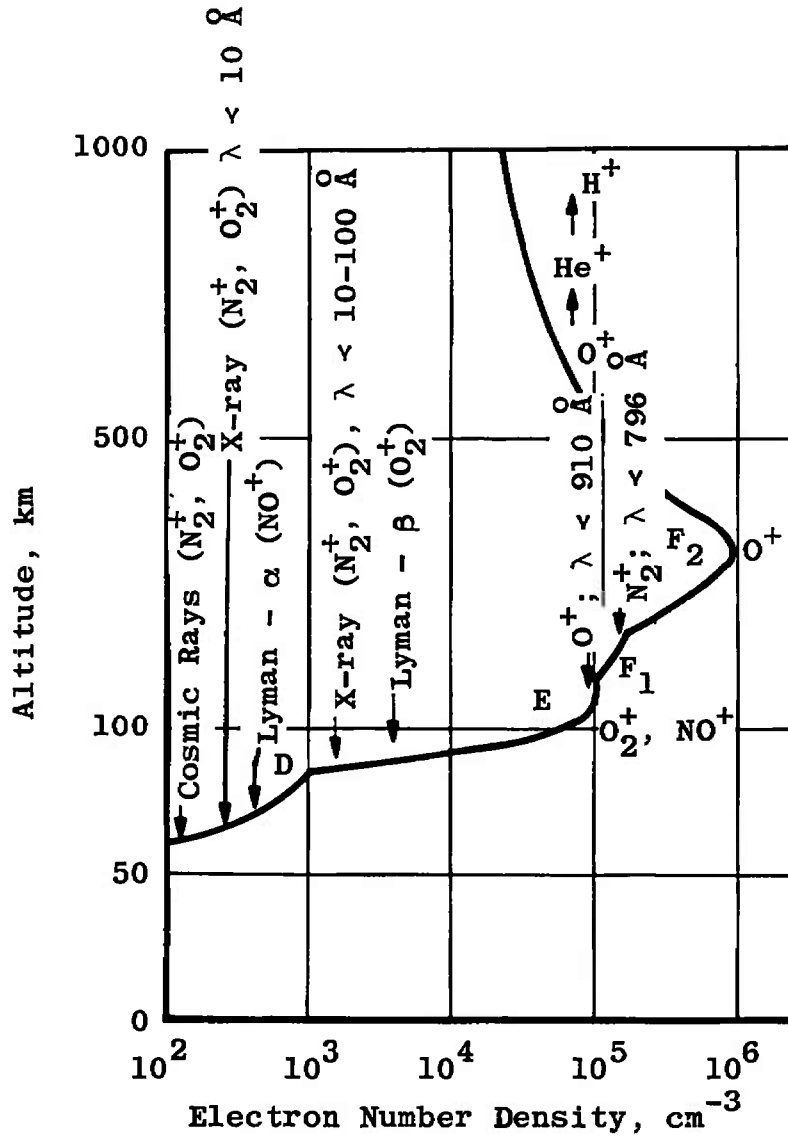
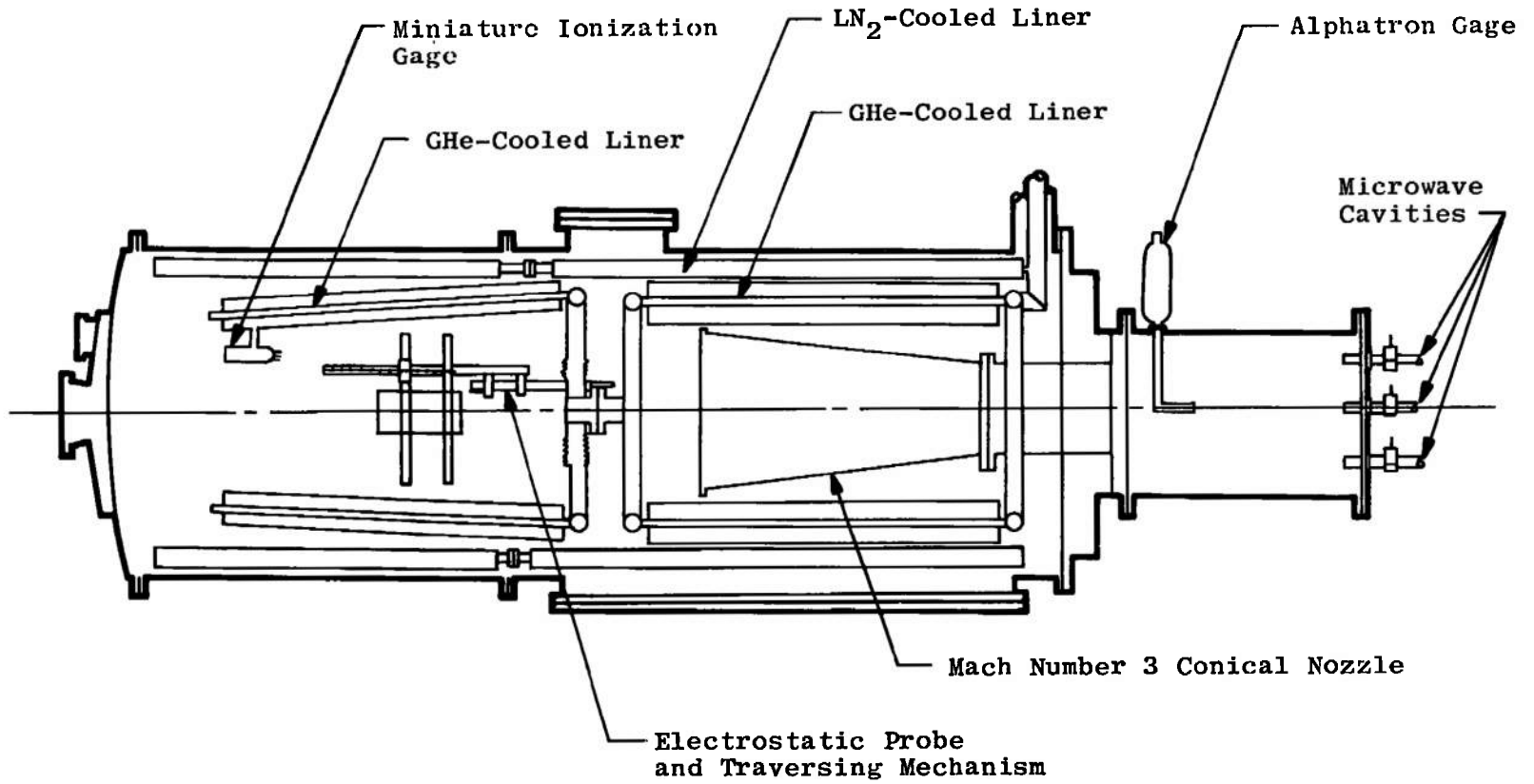


Fig. 1 Typical Electron Distributions in the Ionosphere



16

Fig. 2 Research Vacuum Chamber

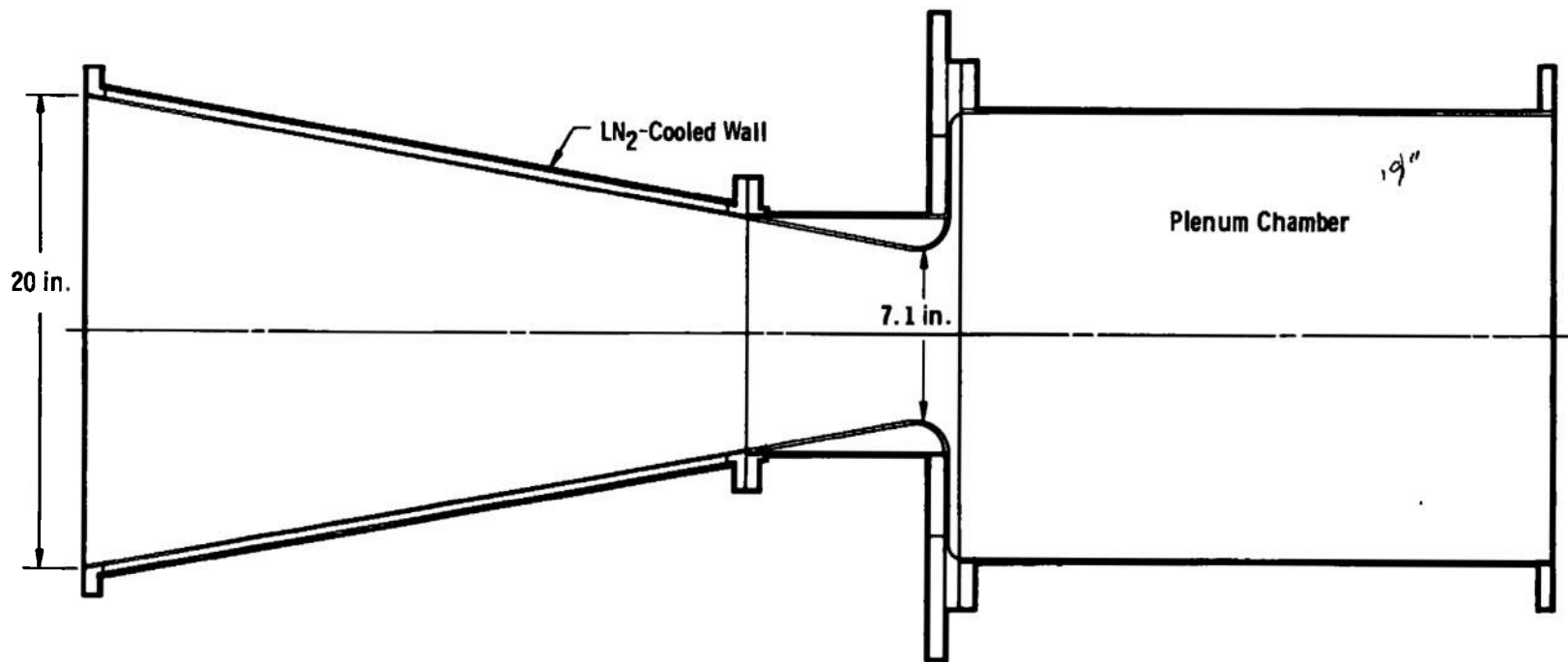


Fig. 3 Mach Number 3 Conical Nozzle

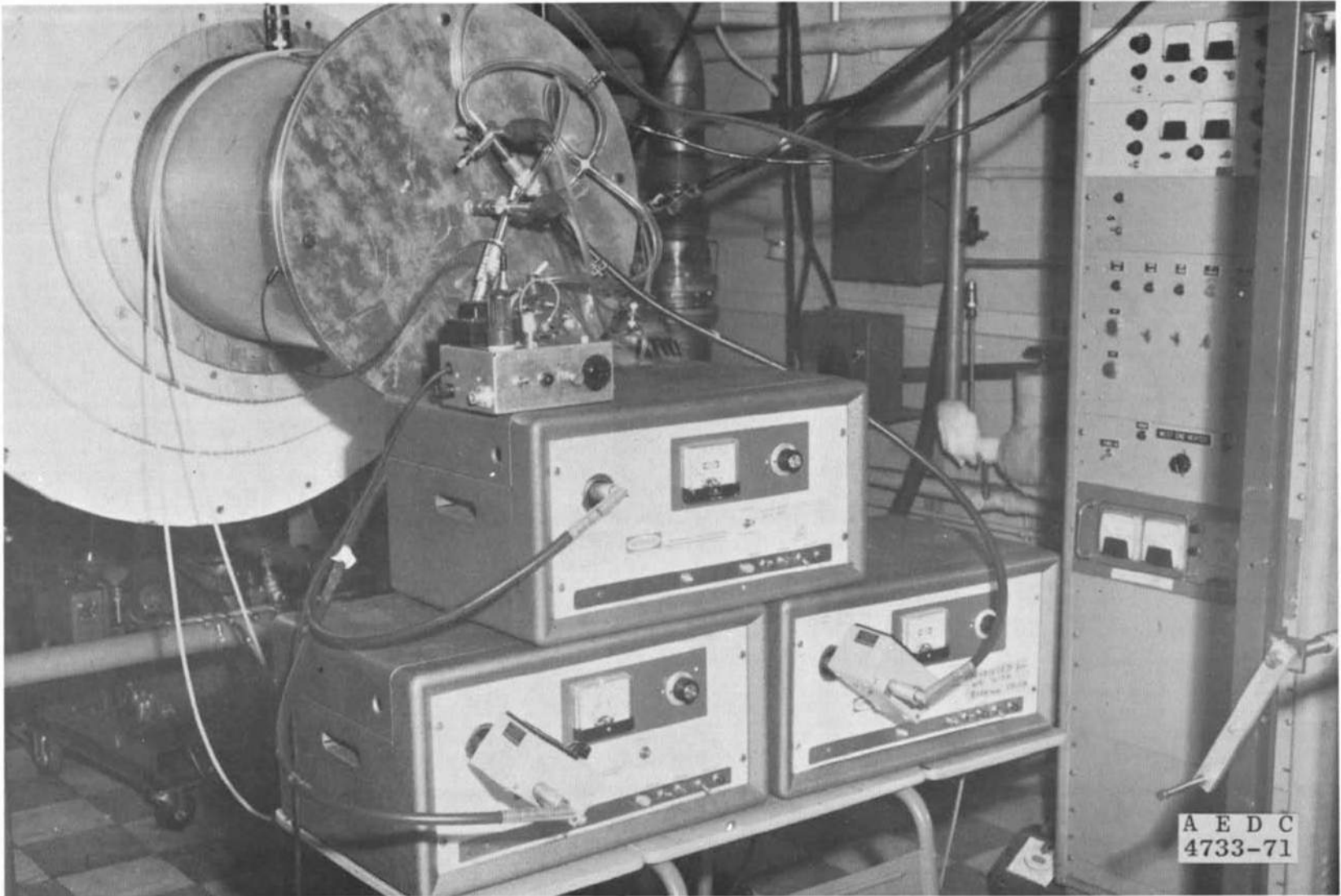


Fig. 4 Gas Addition System and Microwave Generators

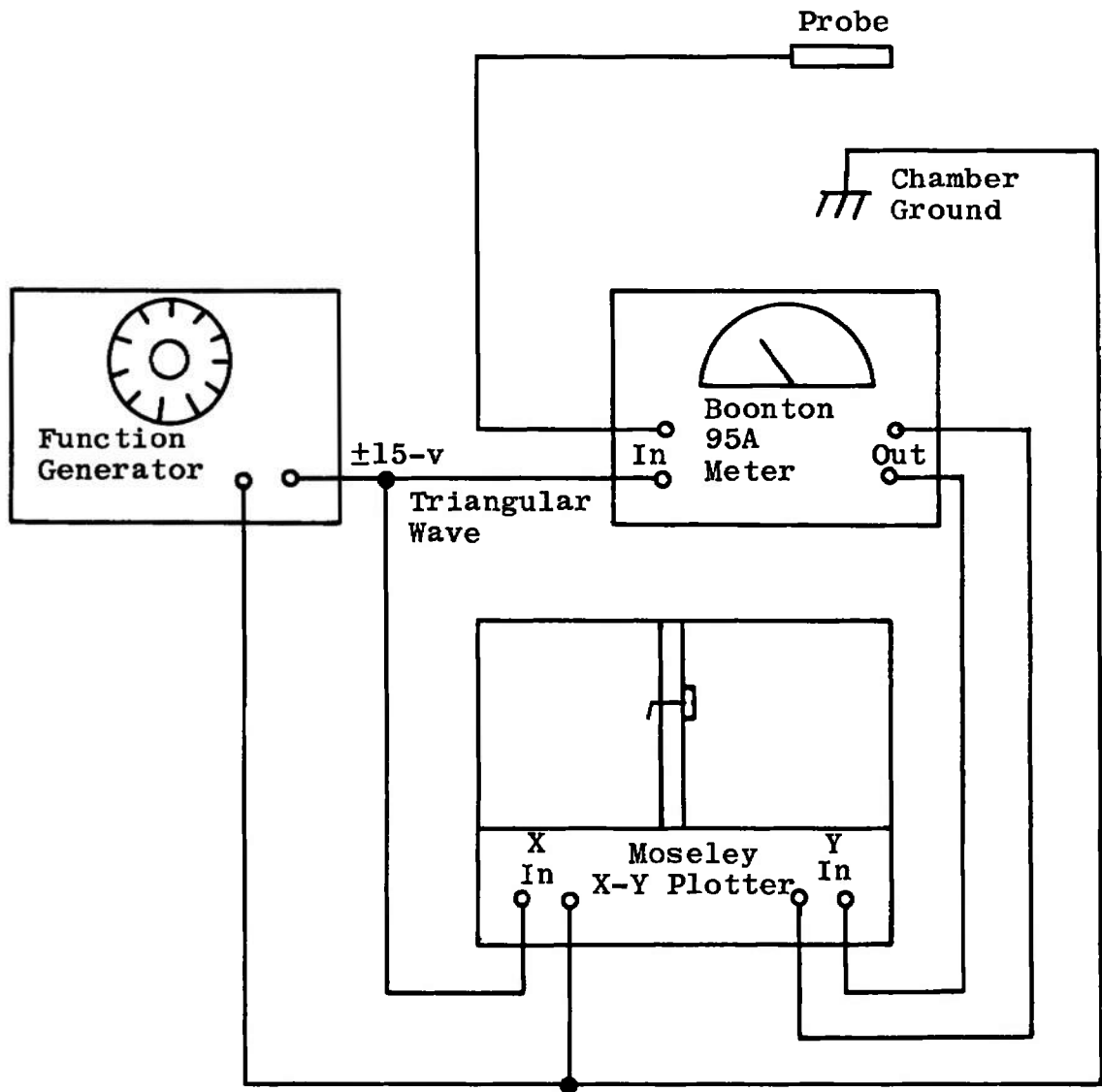


Fig. 5 Schematic of the Electrostatic Probe Instrumentation

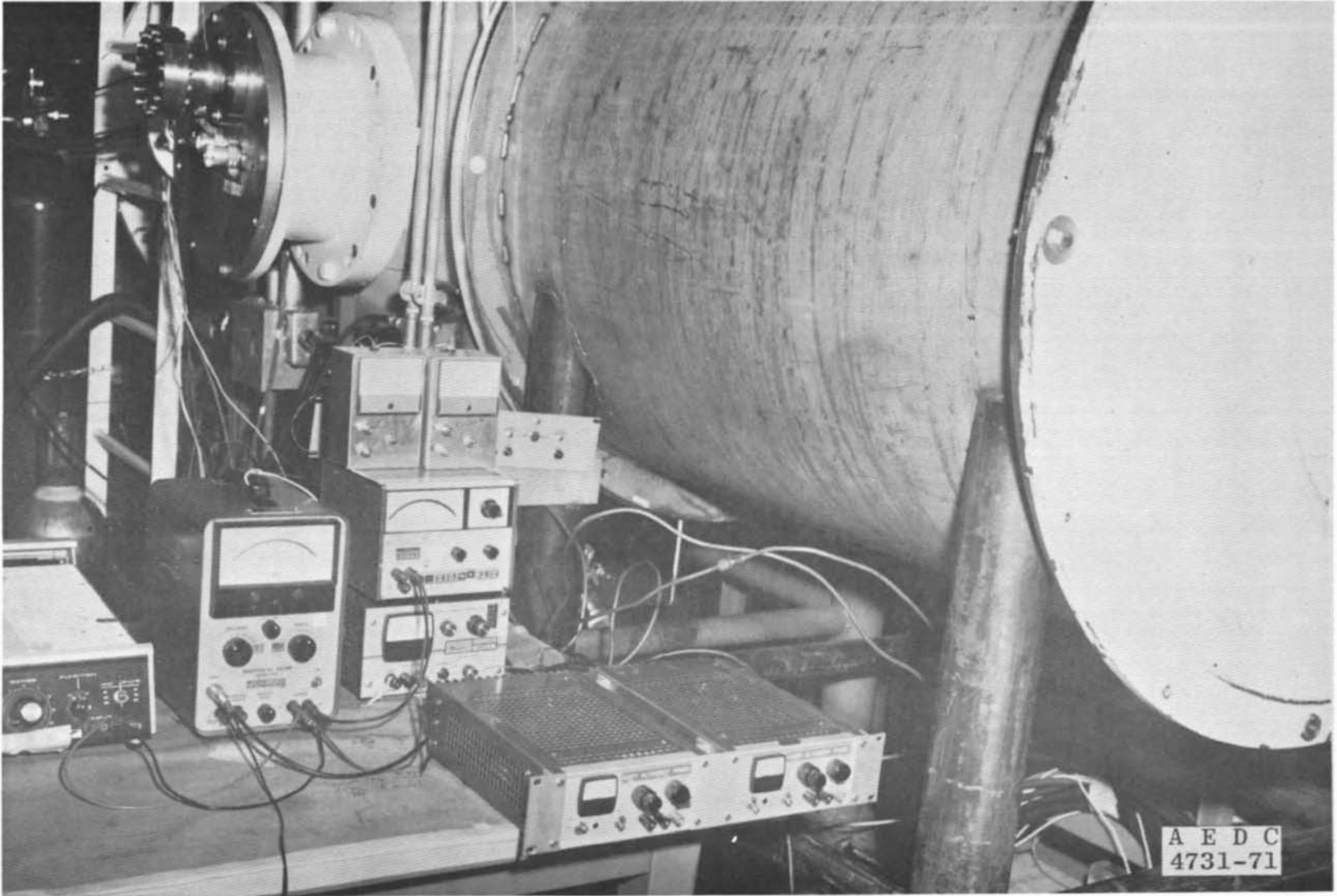


Fig. 6 Electrostatic Probe Instrumentation and Vacuum Cell

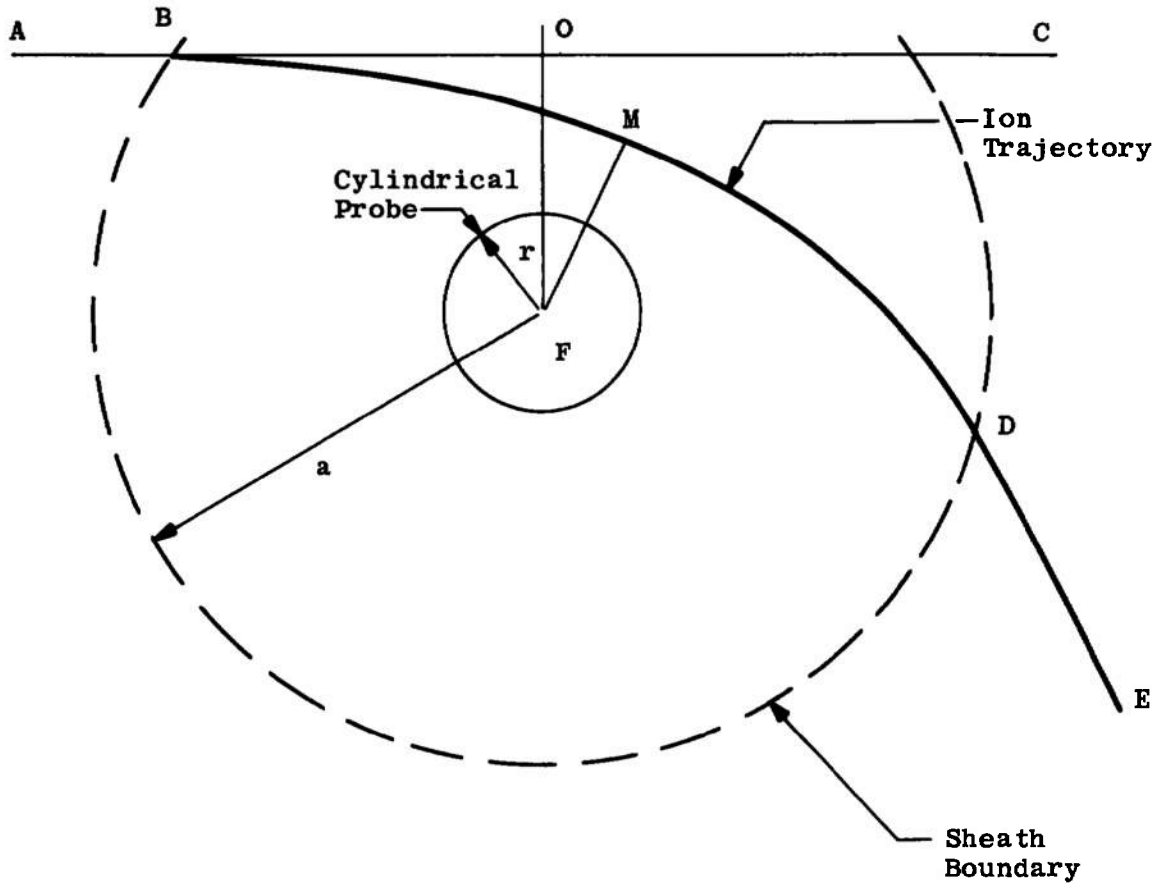


Fig. 7 Path of a Charged Particle Passing through a Sheath Surrounding a Cylinder

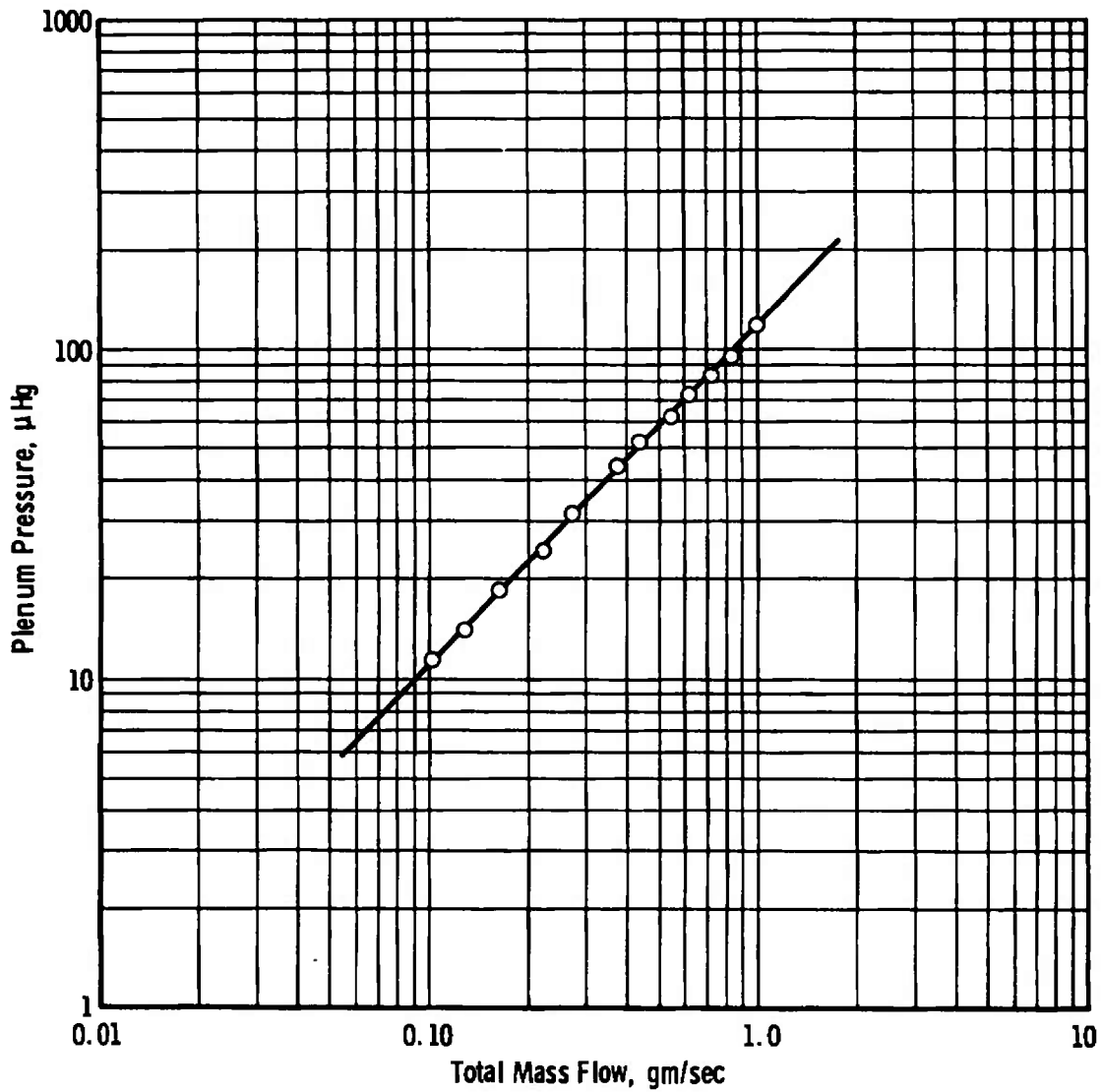


Fig. 8 Total Mass Flow as a Function of Plenum Pressure for the Mach Number 3 Conical Nozzle

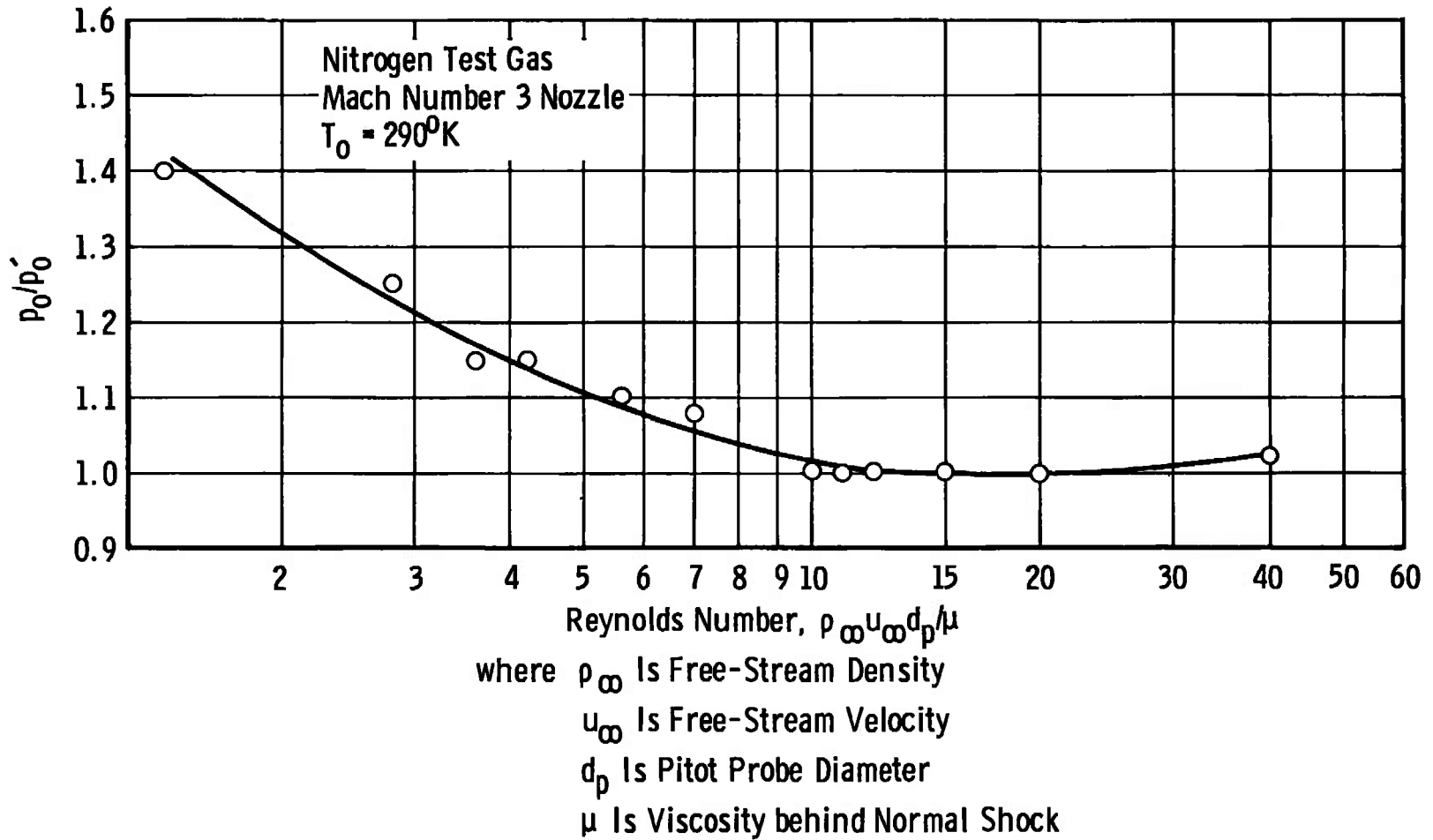


Fig. 9 Pitot Tube Viscous Effect

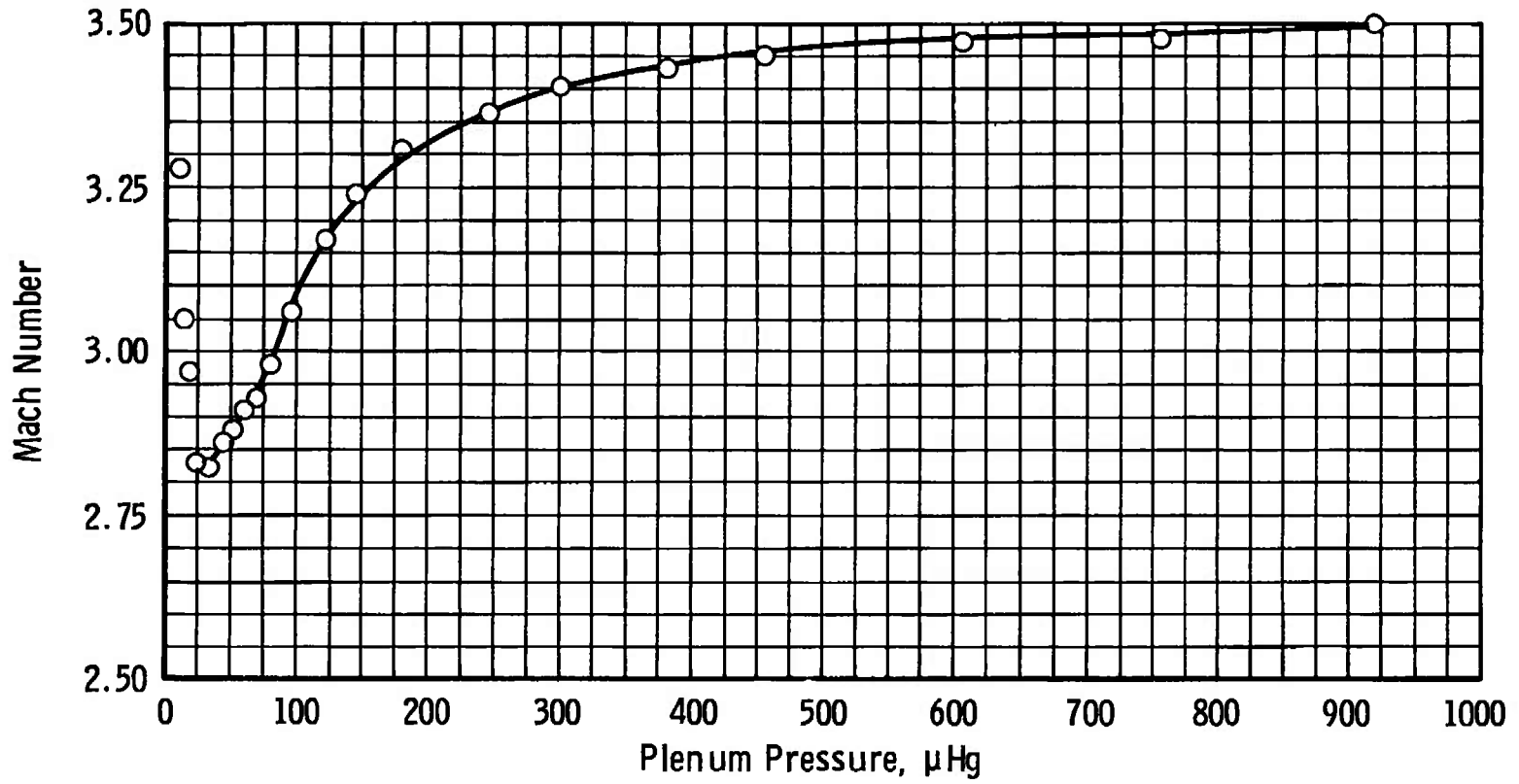


Fig. 10 Mach Number 3 Nozzle Calibration

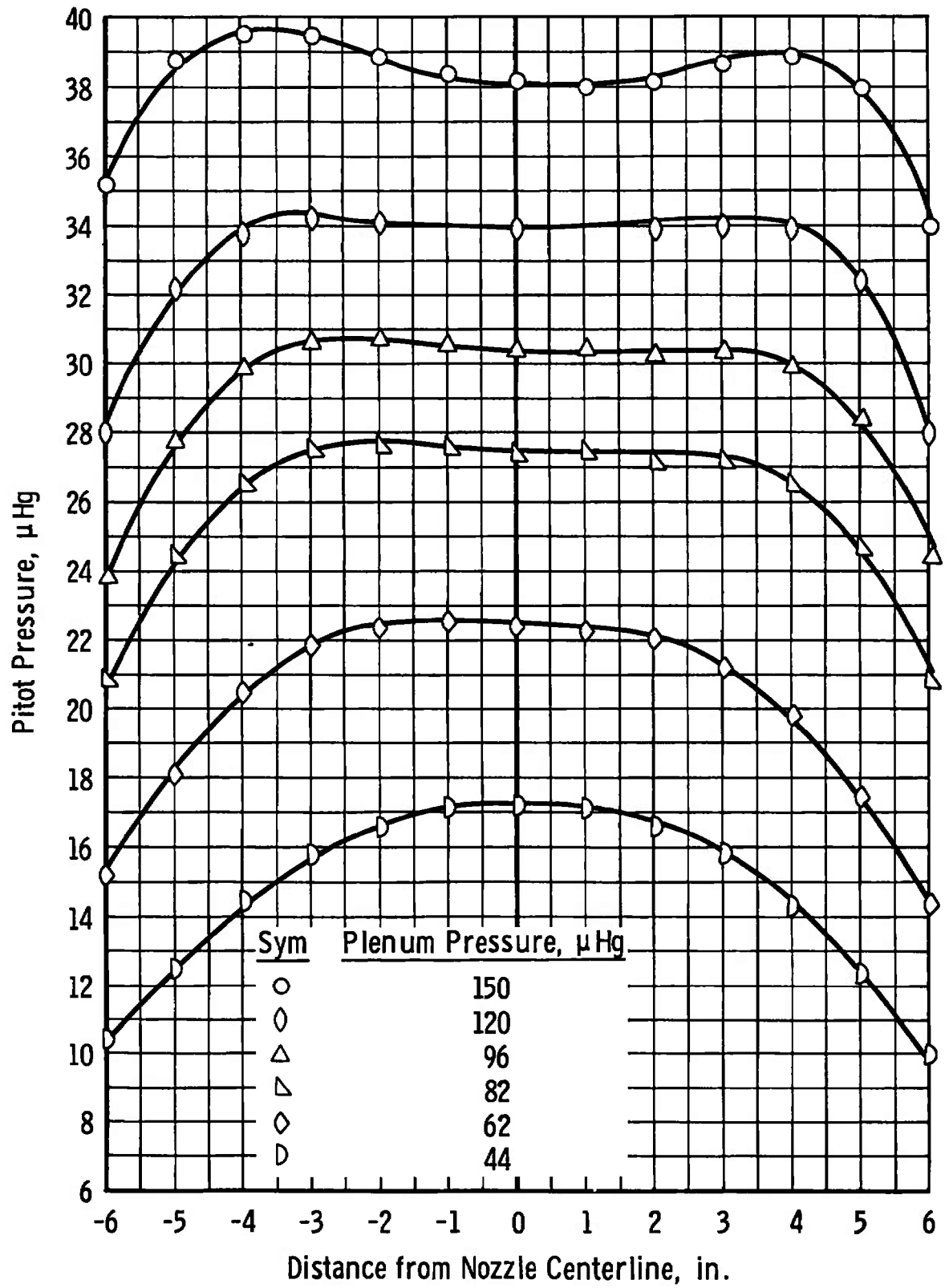


Fig. 11 Pitot Pressure Profiles in Nozzle Exit Plane

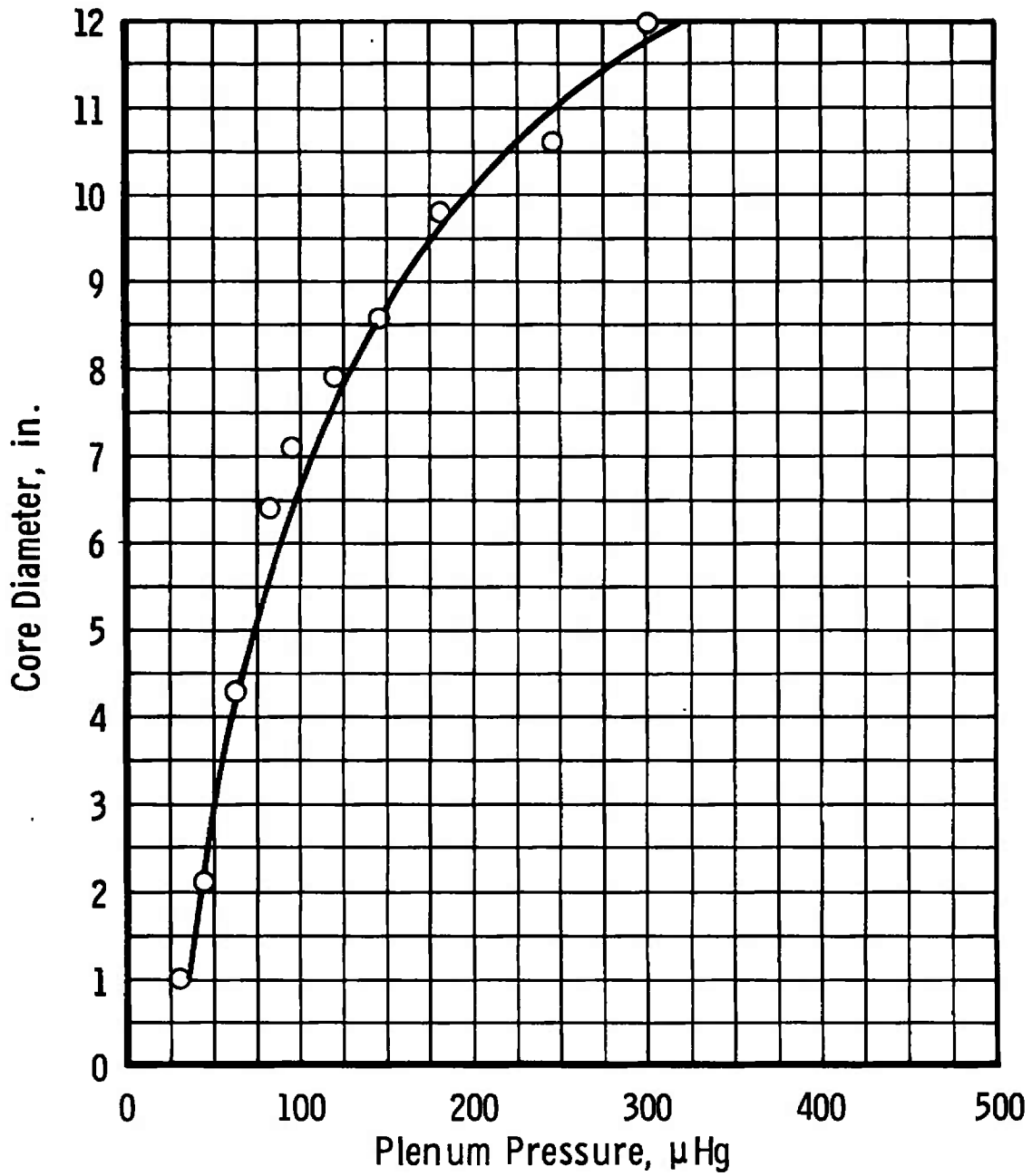


Fig. 12 Nozzle Exit Plane Core Diameter for Various Plenum Pressures

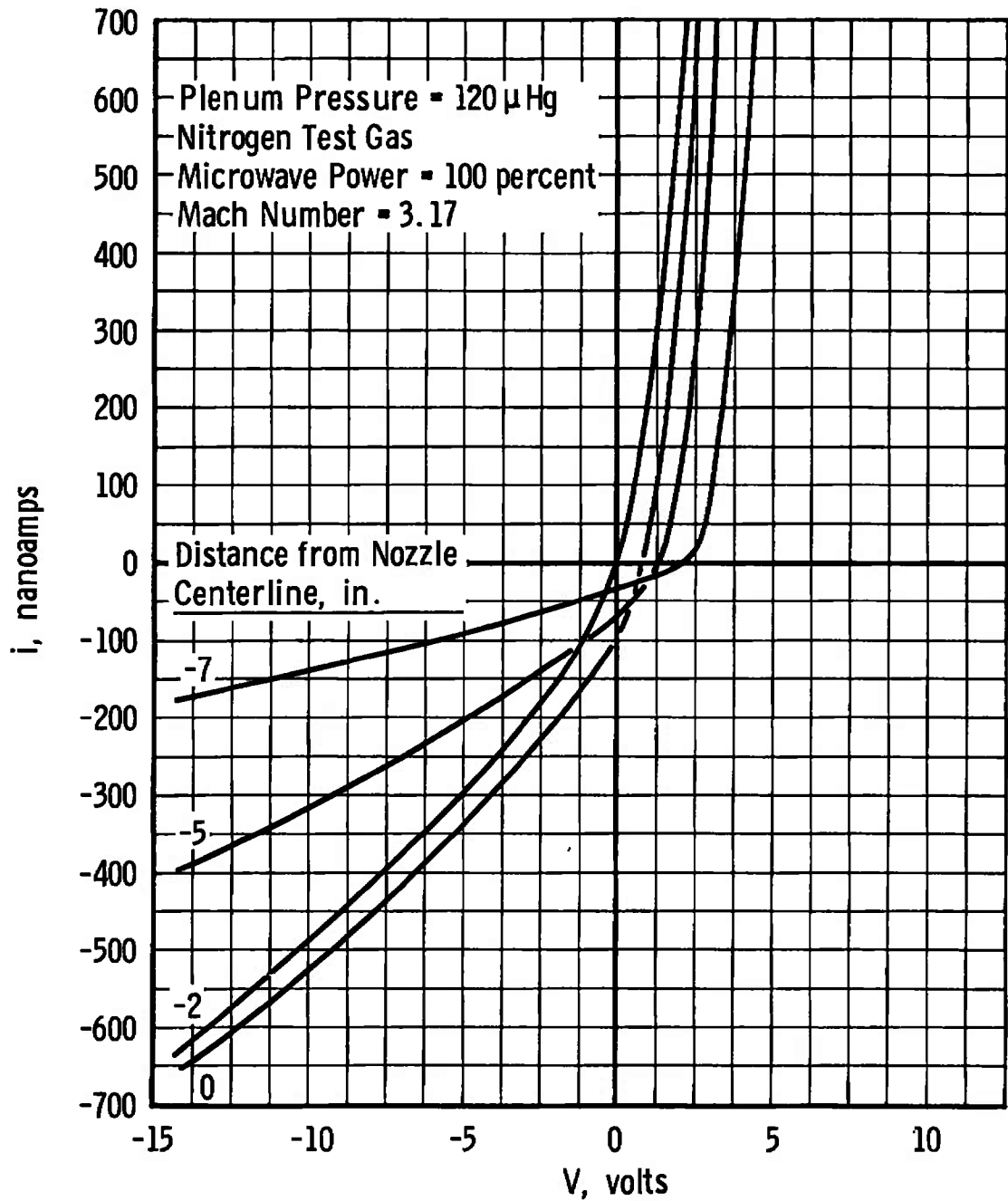


Fig. 13 Voltage-Current Characteristics for Various Probe Positions in Nozzle Exit Plane

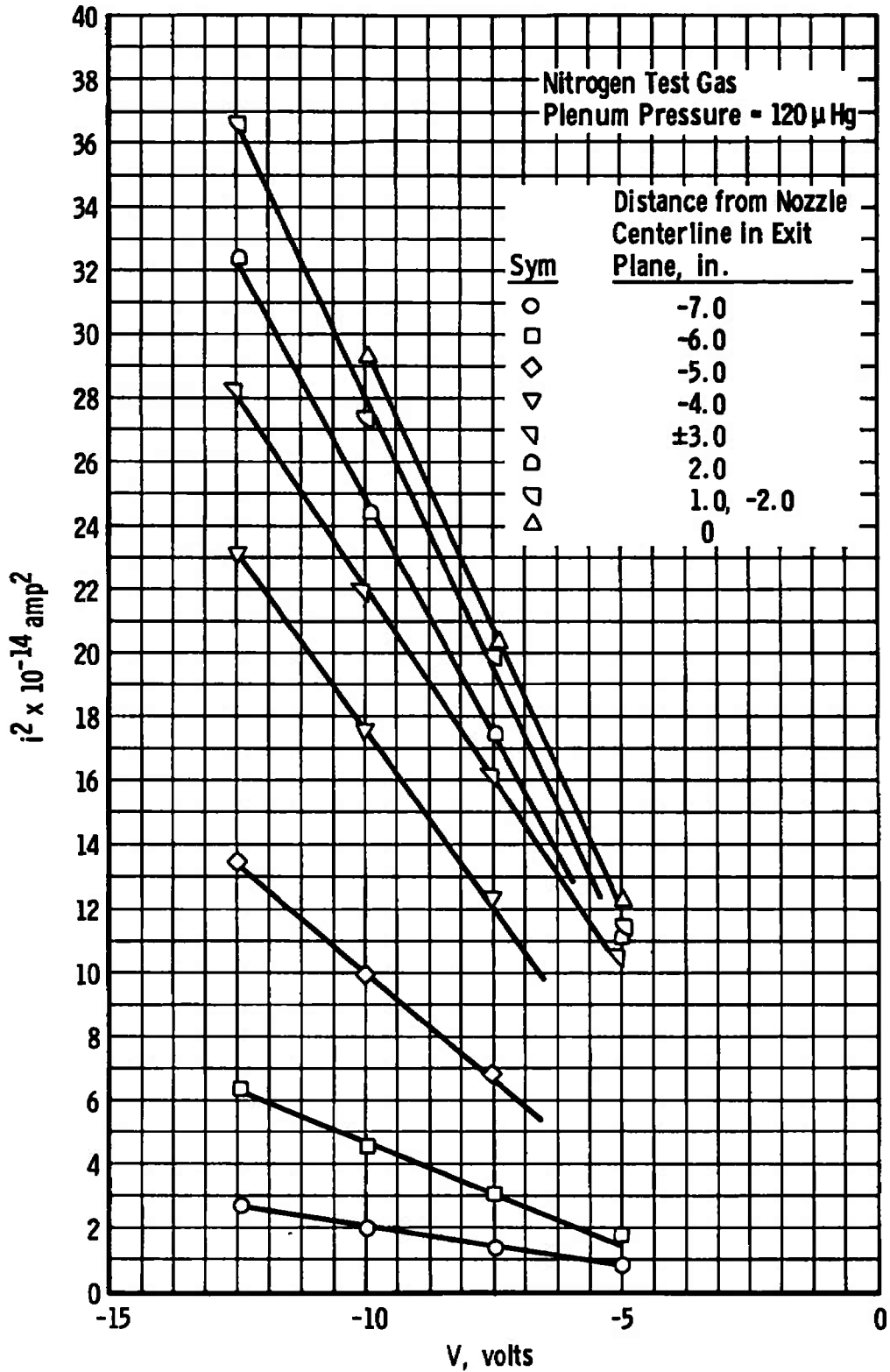


Fig. 14 i^2 -V Curves for Mach Number 3.17 and 100-percent Microwave Power

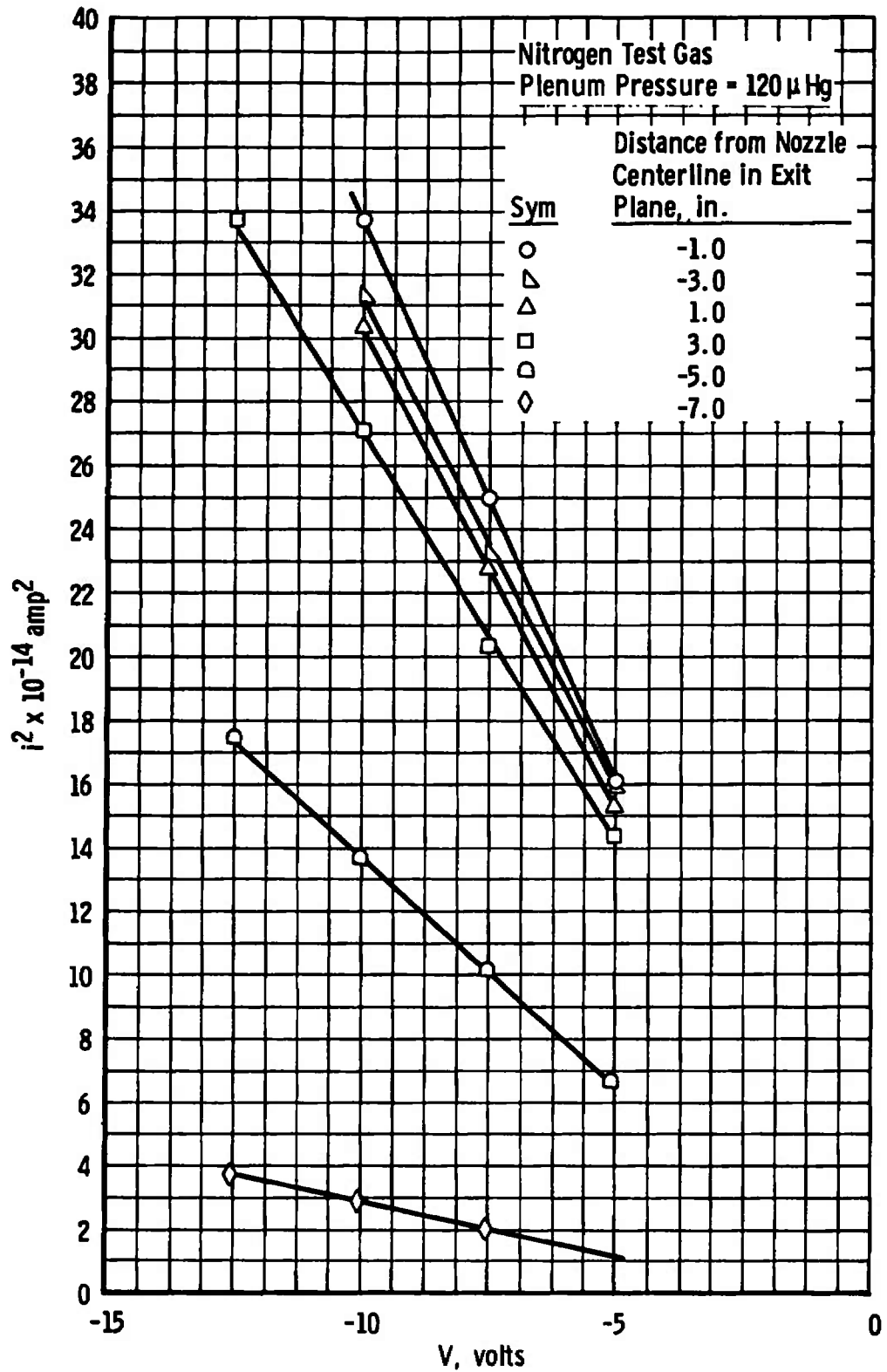


Fig. 15 i^2 -V Curves for Mach Number 3.17 and 75-percent Microwave Power

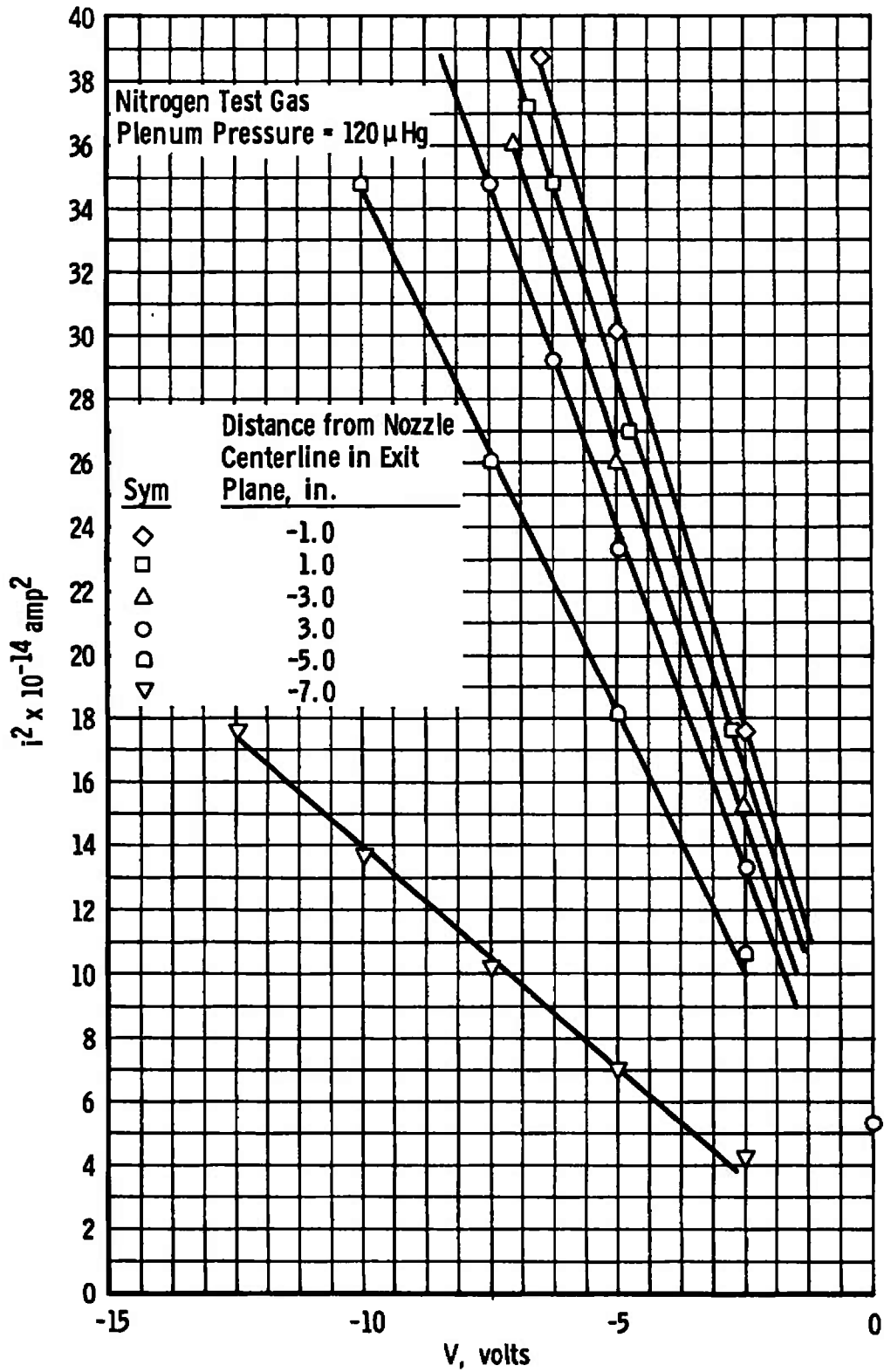


Fig. 16 I^2 -V Curves for Mach Number 3.17 and 50-percent Microwave Power

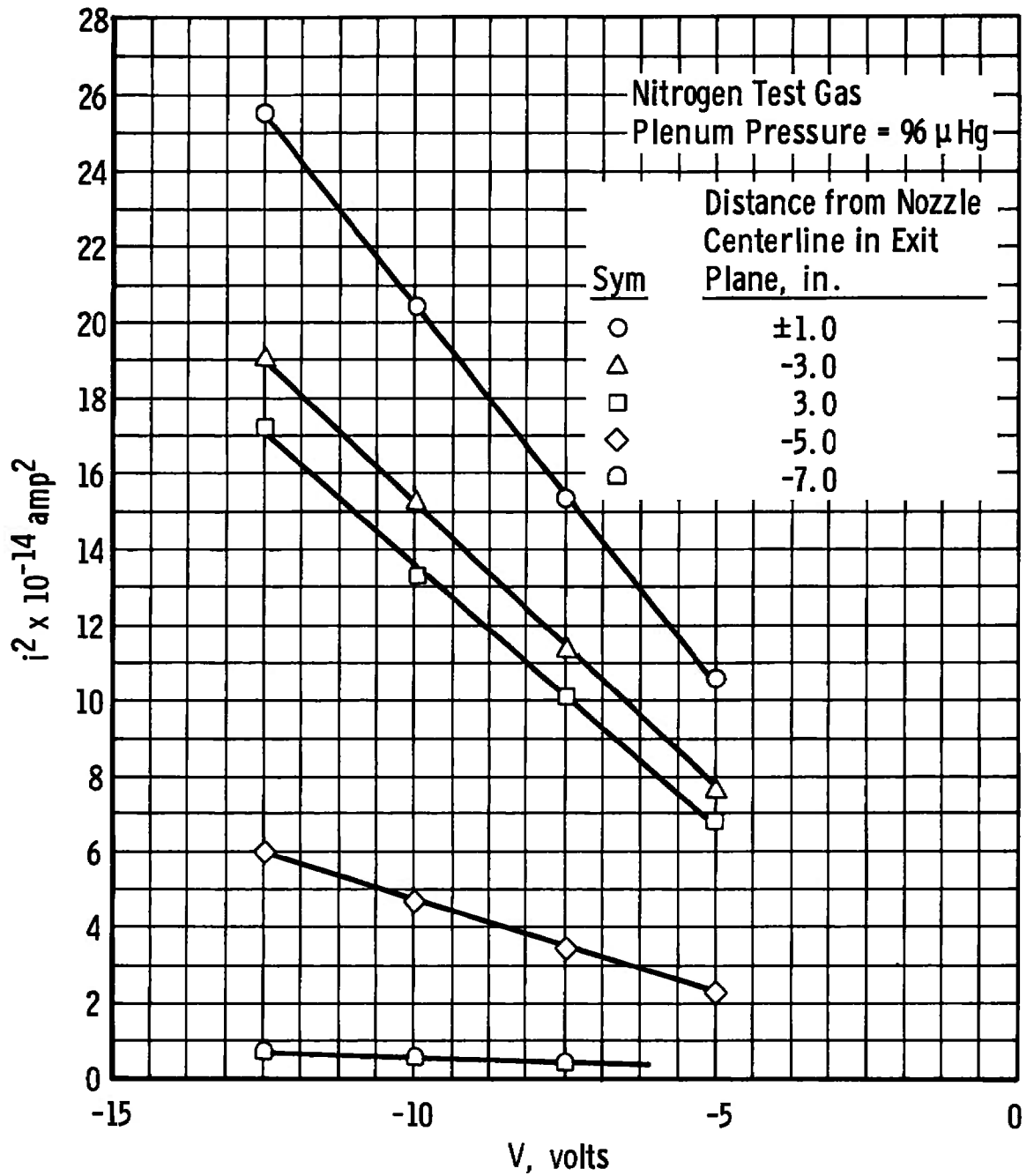


Fig. 17 i^2 -V Curves for Mach Number 3.06 and 100-percent Microwave Power

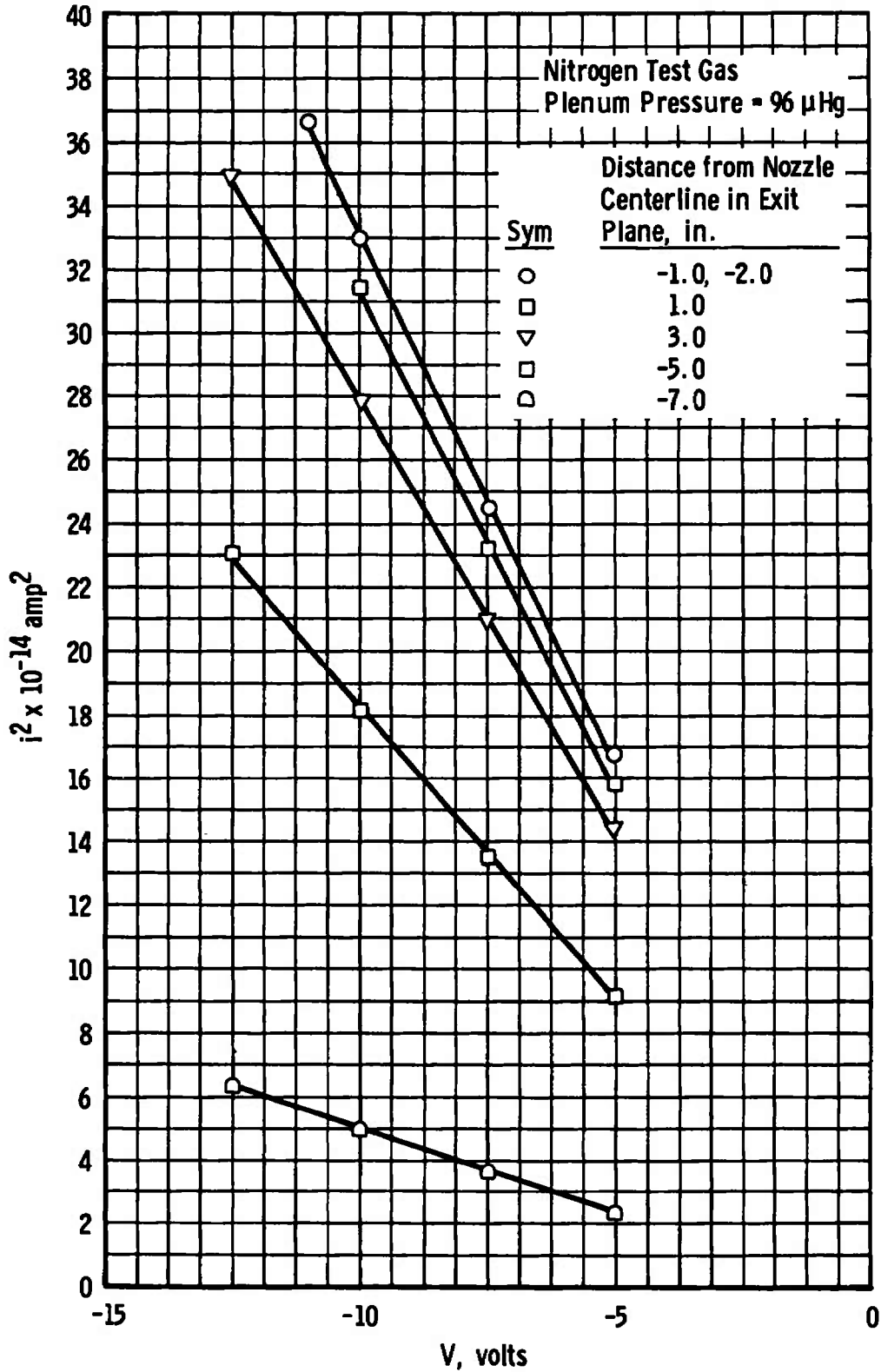


Fig. 18 I^2 -V Curves for Mach Number 3.06 and 50-percent Microwave Power

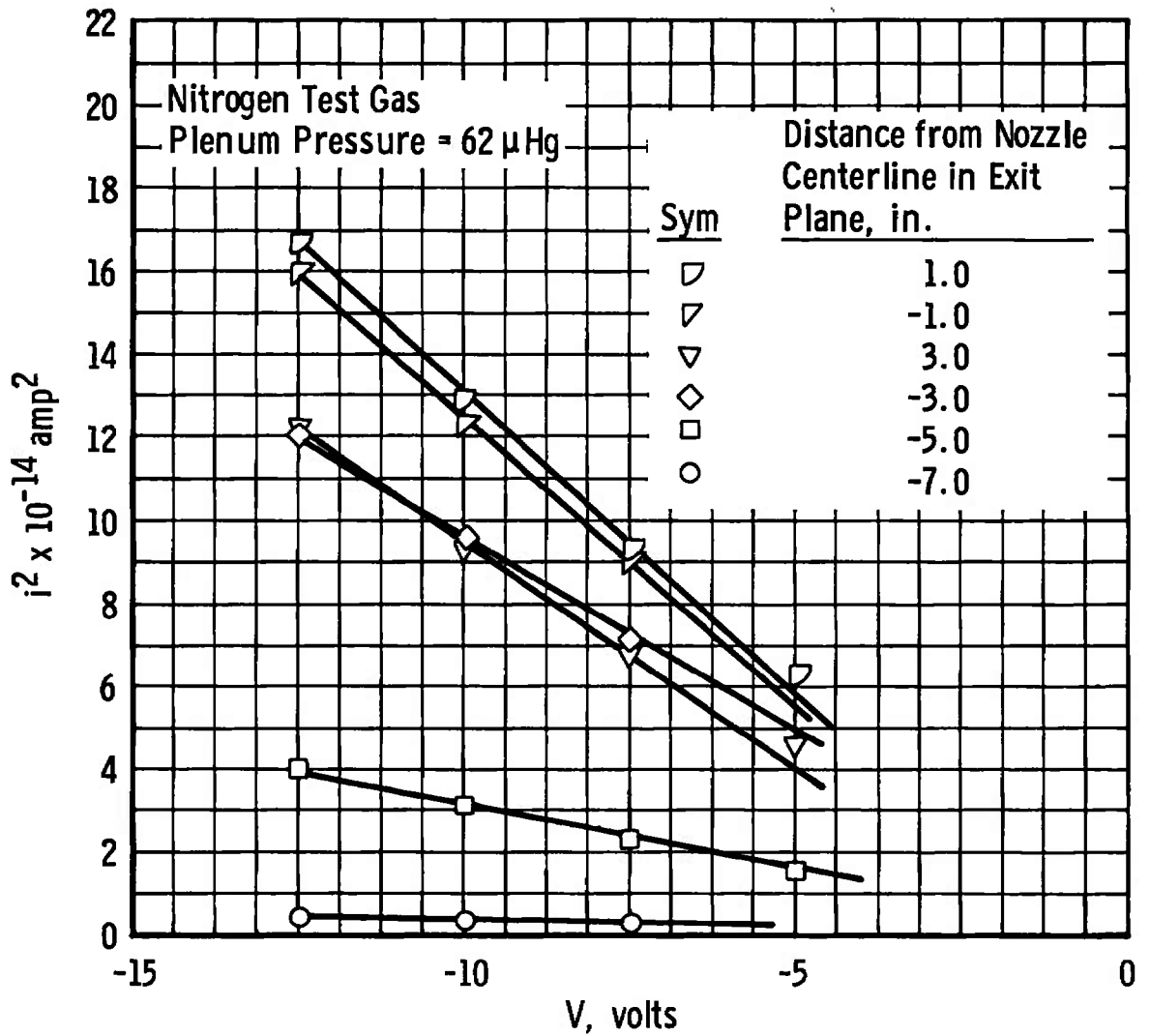


Fig. 19 I^2 -V Curves for Mach Number 2.91 and 100-percent Microwave Power

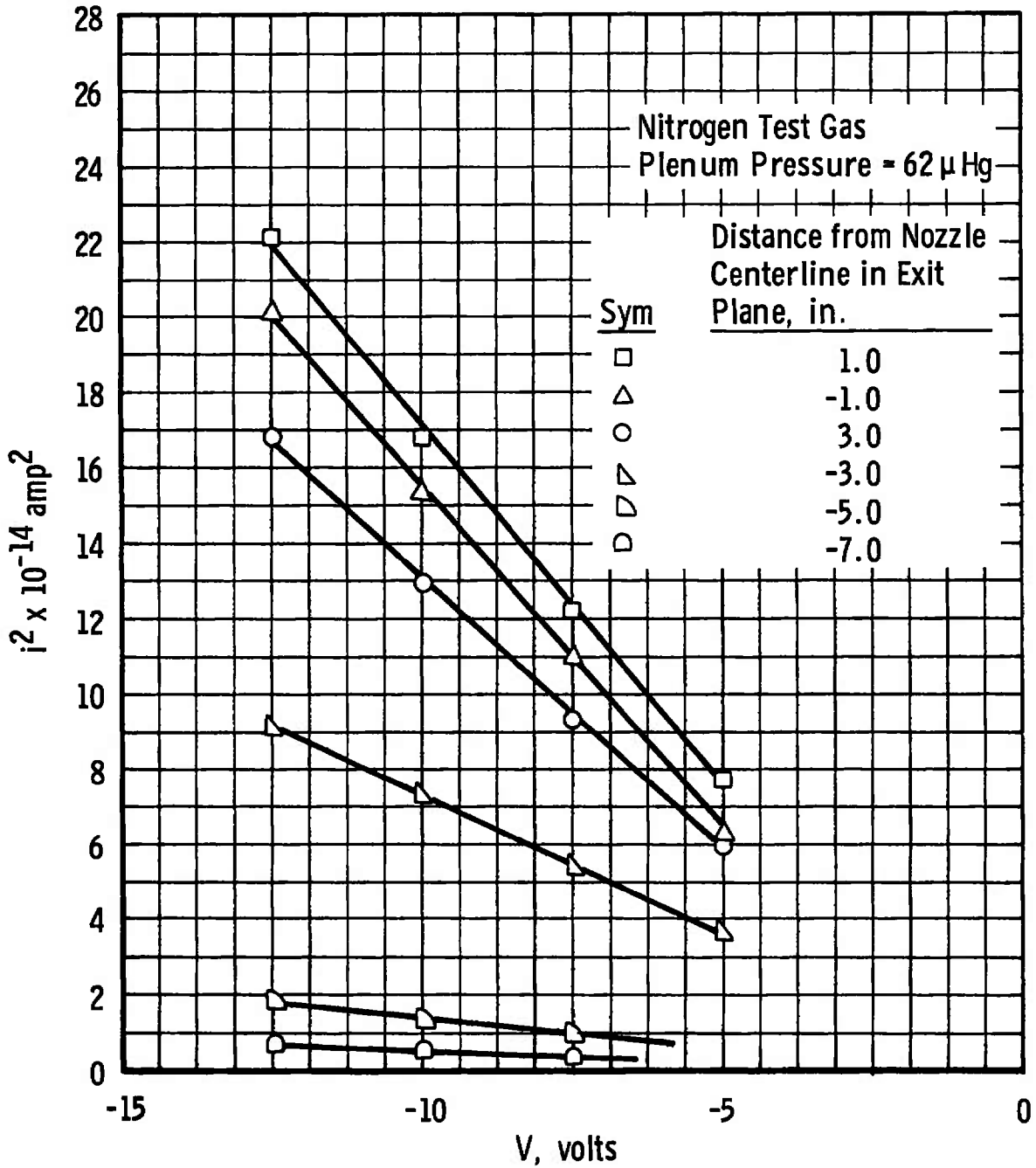


Fig. 20 i^2 -V Curves for Mach Number 2.91 and 50-percent Microwave Power

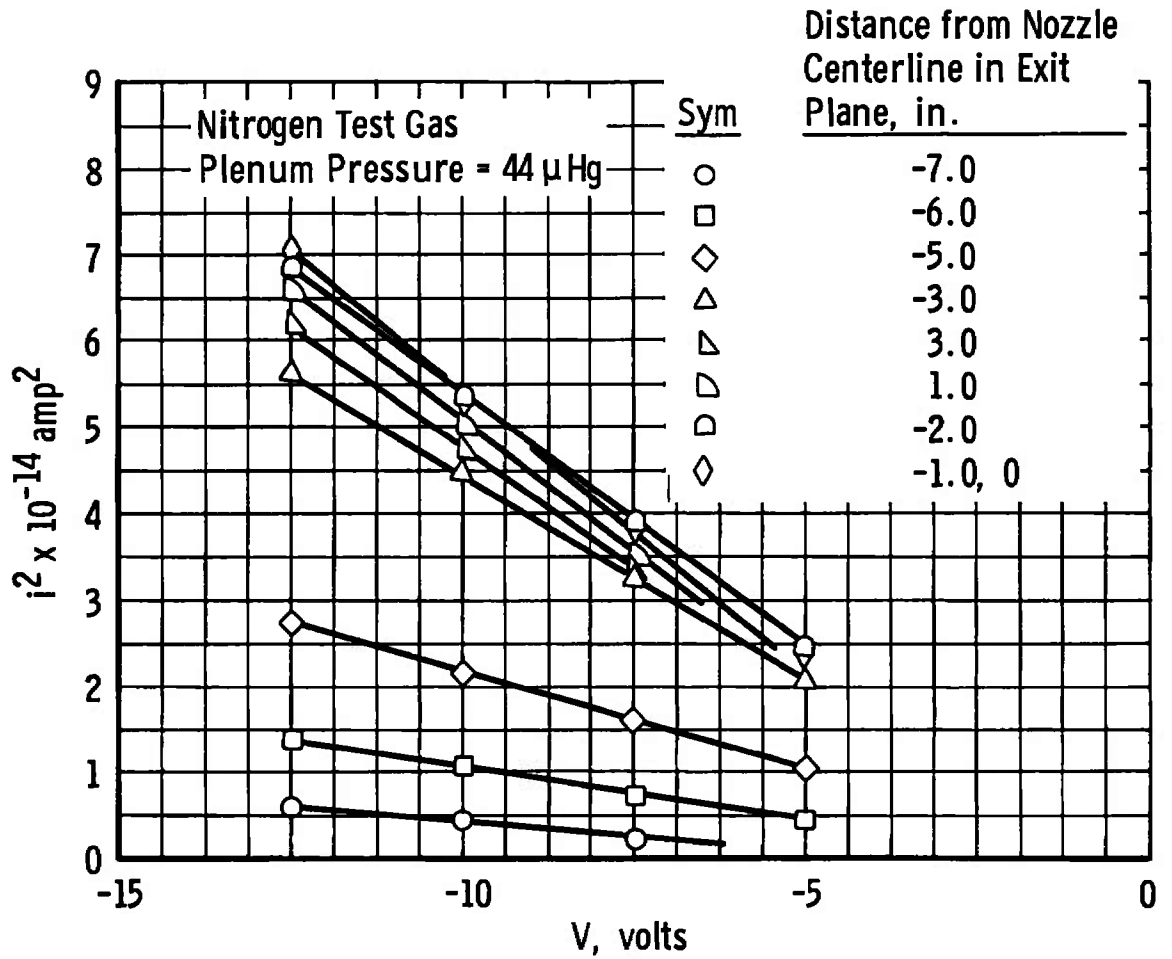


Fig. 21 i^2 -V Curves for Mach Number 2.86 and 100-percent Microwave Power

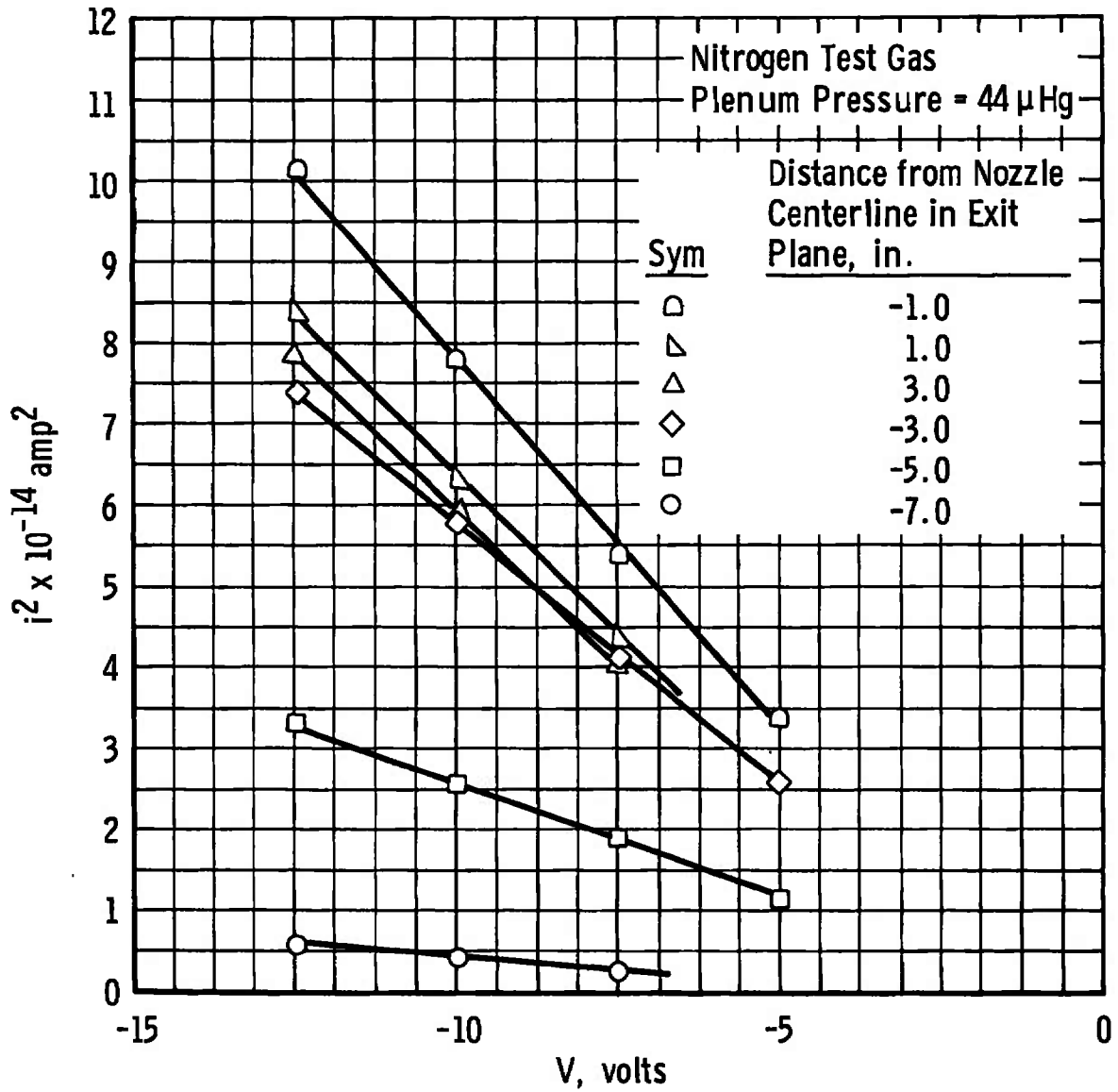


Fig. 22 i^2 -V Curves for Mach Number 2.86 and 50-percent Microwave Power

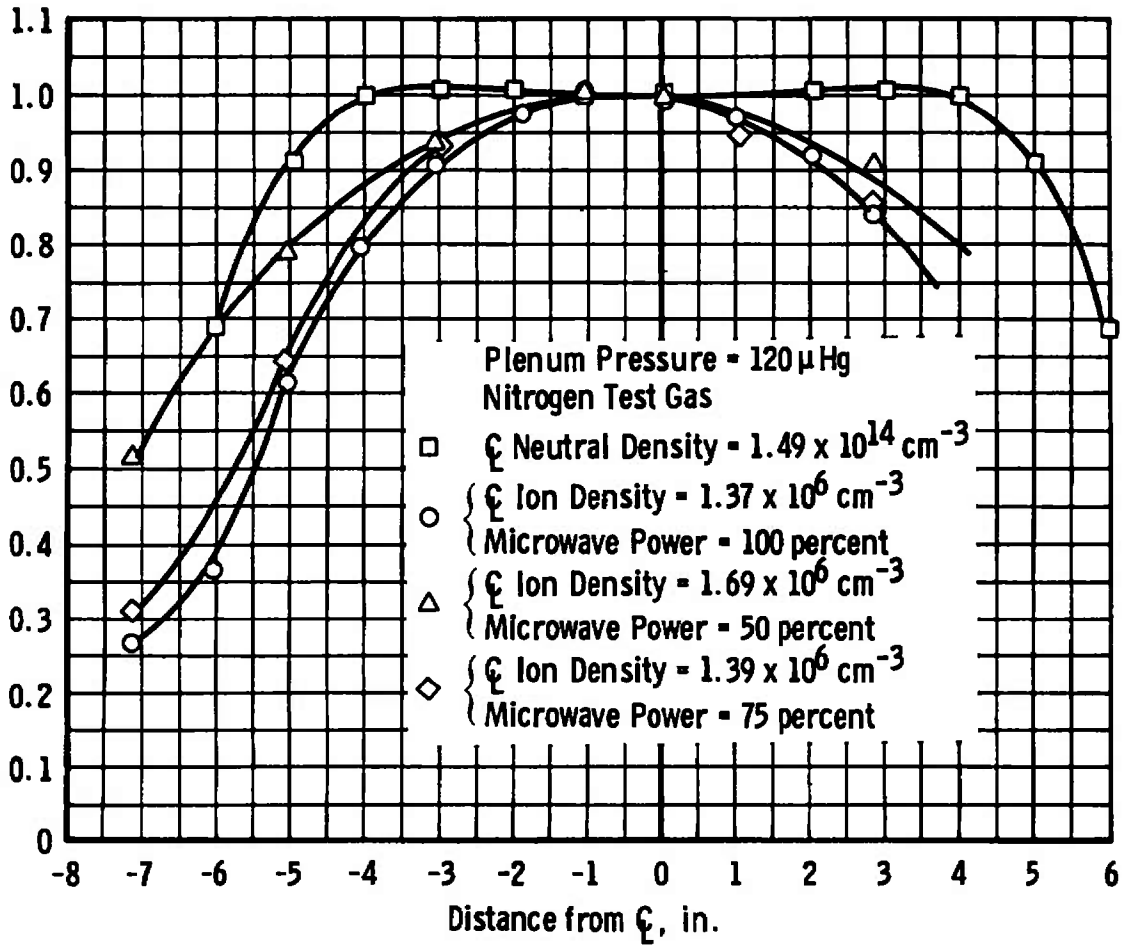


Fig. 23 Normalized Exit Plane Ion Density Profiles for Mach Number 3.17

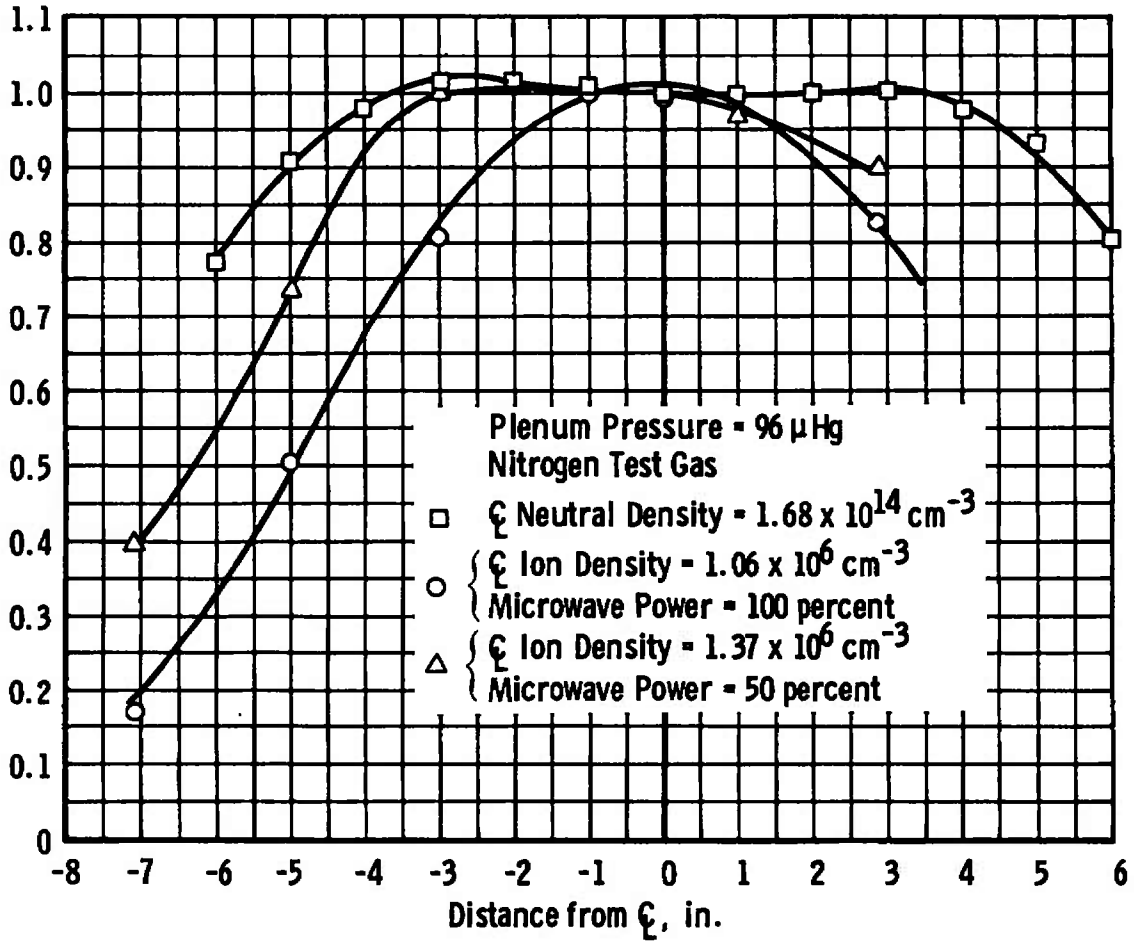


Fig. 24 Normalized Exit Plane Ion Density Profiles for Mach Number 3.06

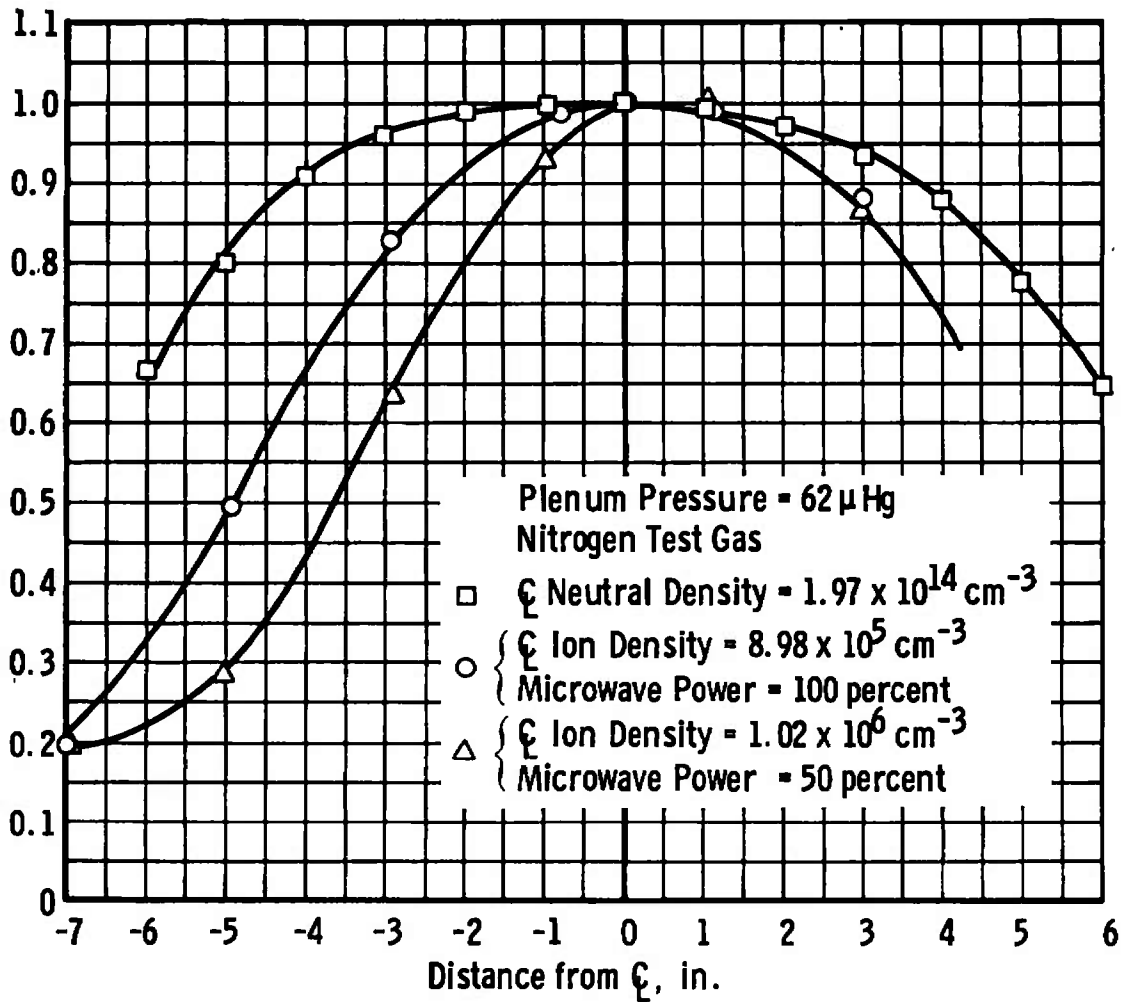


Fig. 25 Normalized Exit Plane Ion Density Profiles for Mach Number 2.91

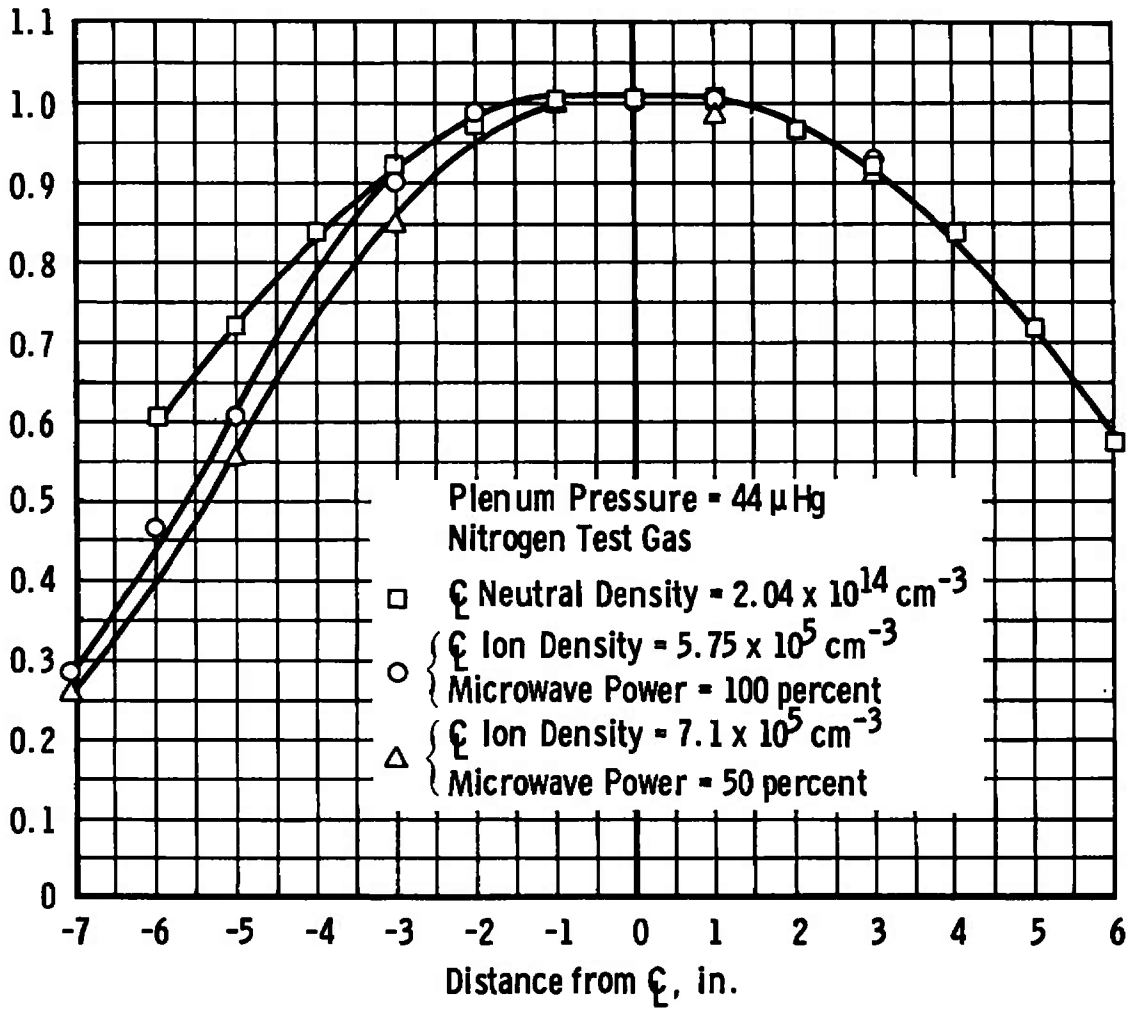


Fig. 26 Normalized Exit Plane Ion Density Profiles for Mach Number 2.86

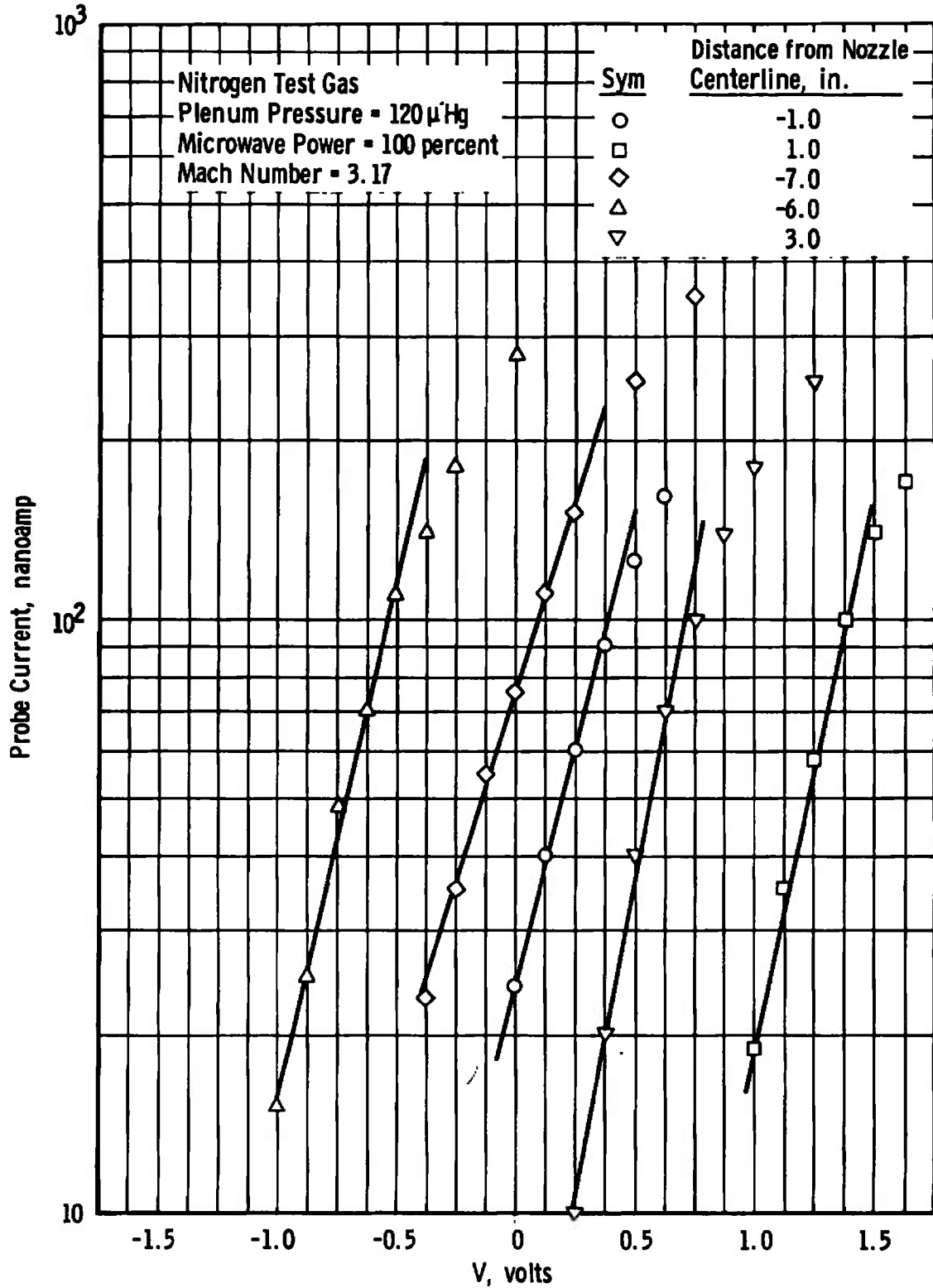


Fig. 27 Nozzle Exit Plane I-V Curves for Various Probe Positions

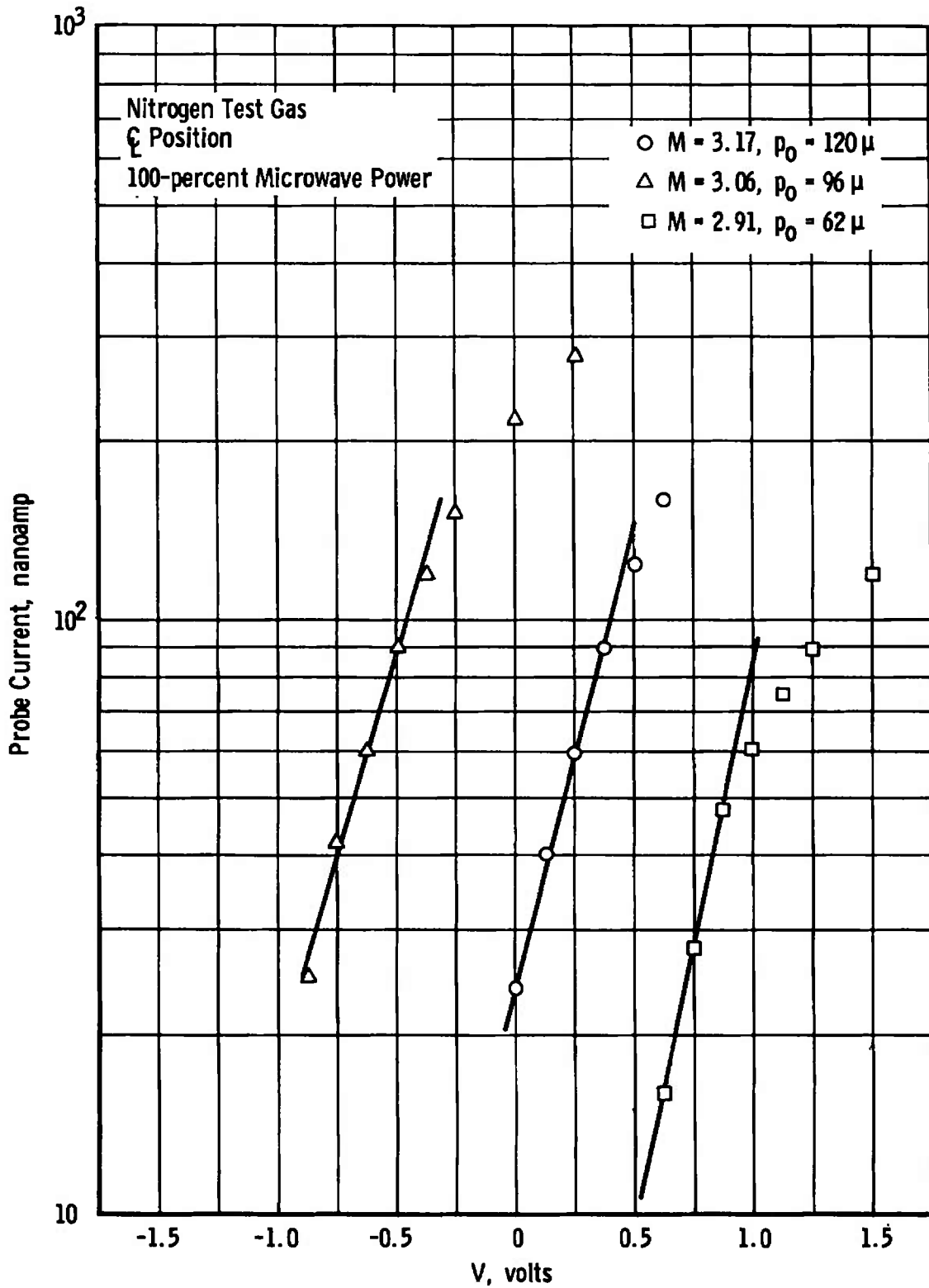


Fig. 28 Nozzle Exit Plane I-V Curves for Various Mach Numbers

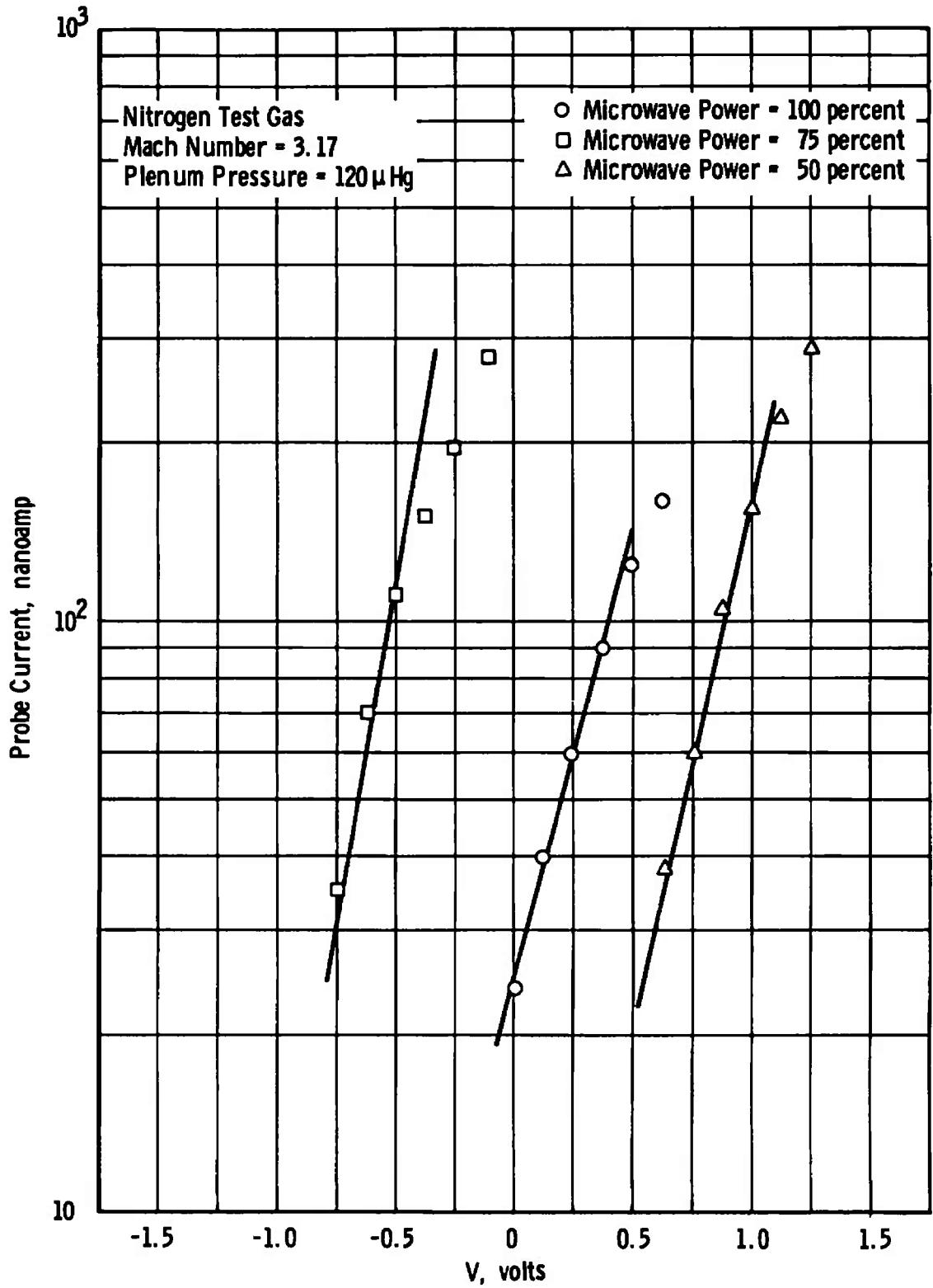


Fig. 29 Nozzle Exit Plane I-V Curves for Various Microwave Powers

TABLE I
CHARACTERISTICS OF THE IONOSPHERE

<u>Height, km</u>	<u>Neutral Density (cm⁻³)</u>	<u>Electron Density (cm⁻³)</u>	<u>Electron Temperature, °K</u>	<u>Mean Molecular Weight</u>
100	3×10^{13}	$(2-100) \times 10^3$	230	28
300	3×10^9	$(1 - 200) \times 10^5$	1000	24
500	5×10^7	$(4 - 10) \times 10^5$	1800	20
700	6×10^6	$(2 - 5) \times 10^5$	2000	16
1000	10^5	10^5	3000	16

TABLE II
**CENTERLINE ION DENSITIES IN THE NOZZLE EXIT PLANE FOR
VARIOUS MICROWAVE POWERS**

<u>Mach Number</u>	<u>Microwave Power, percent</u>	<u>Centerline Ion Densities (cm⁻³)</u>
3.17	100	1.37×10^6
3.17	75	1.39×10^6
3.17	50	1.69×10^6
3.06	100	1.06×10^6
3.06	50	1.36×10^6
2.91	100	8.98×10^5
2.91	50	1.02×10^6
2.86	100	5.75×10^5
2.86	50	7.09×10^5

TABLE III
ESTIMATED ELECTRON TEMPERATURES IN THE
NOZZLE EXIT PLANE FOR MACH NUMBER \approx 3.17

<u>Position,</u> <u>in.</u>	<u>Temperature,</u> <u>°K</u>
-7	3980
-6	2960
-1	3200
1	2760
3	3220

100-percent Microwave Power

TABLE IV
ESTIMATED CENTERLINE ELECTRON TEMPERATURES FOR
VARIOUS MACH NUMBERS IN THE NOZZLE EXIT PLANE

<u>Mach</u> <u>Number</u>	<u>Temperature,</u> <u>°K</u>
3.17	3200
3.06	3700
2.91	2700

100-percent Microwave Power

TABLE V
ESTIMATED CENTERLINE ELECTRON TEMPERATURES FOR
VARIOUS VALUES OF MICROWAVE POWER IN THE NOZZLE EXIT PLANE

Microwave Power, percent	Temperature, °K
100	3200
75	2180
50	2800

Mach Number = 3.17

TABLE VI
COMPARISON OF EXPERIMENTAL RESULTS WITH DESIRED
IONOSPHERE CONDITIONS

	<u>Desired Conditions</u>	<u>Experimental Results</u>
Mach Numbers	2 - 5	2.86 - 3.17
Ion Densities	$10^3 - 10^7$ ions/cm ³	$5.75 \times 10^5 - 1.69 \times 10^6$ ions/cm ³
Electron Temperature	230 - 1800°K	3000°K ± 900°K
Neutral Density	$10^{13} - 10^6$ cm ⁻³	$(1.49 - 2.04) \times 10^{14}$ cm ⁻³

DOCUMENT CONTROL DATA - R & D

(Security classification of title, body of abstract and indexing annotation must be entered when the overall report is classified)

1 ORIGINATING ACTIVITY (Corporate author)

Arnold Engineering Development Center
Arnold Air Force Station, Tennessee

2a. REPORT SECURITY CLASSIFICATION

UNCLASSIFIED

2b. GROUP

N/A

3 REPORT TITLE

SIMULATION OF THE IONOSPHERE UTILIZING MICROWAVE ION GENERATION
TECHNIQUES

4 DESCRIPTIVE NOTES (Type of report and inclusive dates)

March to June 1971 - Final Report

5 AUTHOR(S) (First name, middle initial, last name)

M. R. Busby and B. W. Gilley, ARO, Inc.

6 REPORT DATE

December 1971

7a. TOTAL NO OF PAGES

53

7b. NO OF REFS

5

8a. CONTRACT OR GRANT NO

9a. ORIGINATOR'S REPORT NUMBER(S)

AEDC-TR-71-254

b. PROJECT NO.

c. Program Element 64719F

9b. OTHER REPORT NO(S) (Any other numbers that may be assigned
this report)

ARO-VKF-TR-71-180

d.

10 DISTRIBUTION STATEMENT

Approved for public release; distribution unlimited.

11. SUPPLEMENTARY NOTES

Available in DDC

12. SPONSORING MILITARY ACTIVITY

Arnold Engineering Development
Center, Air Force Systems Command,
Arnold AF Station, Tenn. 37389

13. ABSTRACT

An experimental investigation of the simulation of the environment encountered in the lower regions of the ionosphere (50 to 500 km) has been conducted at AEDC. Microwave cavities were utilized in conjunction with a converging-diverging nozzle and a cryogenically pumped vacuum chamber to produce supersonic flow fields with small ion number densities. A platinum, cylindrical, electrostatic probe was used to measure the voltage-current characteristics of the low density plasma in the nozzle exit plane. For exit plane Mach numbers of 2.86 to 3.17, ion densities of $5.75 \times 10^5 \text{ cm}^{-3}$ to $1.69 \times 10^6 \text{ cm}^{-3}$ and electron temperatures of $3000^\circ\text{K} \pm 900^\circ\text{K}$ were calculated using the electrostatic probe characteristics.

14.

KEY WORDS

simulation
ionosphere
microwave
ion density
electrostatic probes
electron energy
Mach numbers

LINK A

LINK B

LINK C

ROLE

WT

ROLE

WT

ROLE

WT